Bioorganic & Medicinal Chemistry 24 (2016) 1793–1810

Contents lists available at ScienceDirect

Bioorganic & Medicinal Chemistry

journal homepage: www.elsevier.com/locate/bmc

Design, physico-chemical properties and biological evaluation of some new *N*-[(phenoxy)alkyl]- and *N*-{2-[2-(phenoxy)ethoxy]ethyl}aminoalkanols as anticonvulsant agents

A. M. Waszkielewicz [a,*], A. Gunia-Krzyżak [a], B. Powroźnik [b], K. Słoczyńska [b], E. Pękala [b], M. Walczak [c], M. Bednarski [d], E. Żesławska [e], W. Nitek [f], H. Marona [a]

[a] Department of Bioorganic Chemistry, Faculty of Pharmacy, Jagiellonian University Medical College, Medyczna 9, 30-688 Krakow, Poland
[b] Department of Pharmaceutical Biochemistry, Faculty of Pharmacy, Jagiellonian University Medical College, Medyczna 9, 30-688 Krakow, Poland
[c] Department of Toxicology, Faculty of Pharmacy, Jagiellonian University Medical College, Medyczna 9, 30-688 Krakow, Poland
[d] Laboratory of Pharmacological Screening, Faculty of Pharmacy, Jagiellonian University Medical College, Medyczna 9, 30-688 Krakow, Poland
[e] Department of Chemistry, Institute of Biology, Pedagogical University, Podchorążych 2, 30-084 Krakow, Poland
[f] Faculty of Chemistry, Jagiellonian University, Ingardena 3, 30-060 Krakow, Poland

ARTICLE INFO

Article history:
Received 28 January 2016
Revised 1 March 2016
Accepted 2 March 2016
Available online 3 March 2016

Dedicated to the memory of Professor Jan Krzek

Keywords:
Aminoalkanols
Anticonvulsant activity
Seizures
Sigma receptors
5-HT
MES
Metabolic stability
Mutagenicity
Vibrio harveyi
Pharmacokinetics

ABSTRACT

A series of thirty *N*-(phenoxy)alkyl or *N*-{2-[2-(phenoxy)ethoxy]ethyl}aminoalkanols has been designed, synthesized and evaluated for anticonvulsant activity in MES, 6 Hz test, and pilocarpine-induced status epilepticus. Among the title compounds, the most promising seems *R*-(−)-2*N*-{2-[2-(2,6-dimethylphenoxy)ethoxy]ethyl}aminopropan-1-ol hydrochloride (**22a**) with proved absolute configuration with X-ray analysis and enantiomeric purity. The compound is effective in MES test with ED_{50} = 12.92 mg/kg b.w. and its rotarod TD_{50} = 33.26 mg/kg b.w. The activity dose is also effective in a neurogenic pain model—the formalin test. Within high throughput profile assay, among eighty one targets, the strongest affinity of the compound is observed towards σ receptors and 5-HT transporter and the compound does not bind to hERG. It also does not exhibit mutagenic properties in the *Vibrio harveyi* test. Moreover, murine liver microsomal assay and pharmacokinetics profile (mice, *iv*, *p.o.*, *ip*) indicate that the liver is the primary site of biotransformation of the compound, suggesting that both **22a** and its metabolite(s) are active, compensating probably low bioavailability of the parent molecule.

© 2016 Elsevier Ltd. All rights reserved.

1. Introduction

Epilepsy constitutes one of major neurological disorders—it is a set of disorders having in common hypersynchronous discharges in neurons. Overall incidence of epilepsy is estimated 50 per 100,000/year. The variety of types of seizures causes situation that particular patients suffer from drug resistant seizures, which constitute about 30% of cases. Moreover, toxicity and adverse reactions of anticonvulsants are a significant cause for self-discontinuation of treatment by patients, especially during pregnancy.[1] Therefore, despite large progress in antiepileptic drug development, there are still premises for search of new anticonvulsant compounds which will be both effective and safe.[2]

Antiepileptic drugs belong to many chemical groups, exhibit various activity, and therefore are used in various types of seizures. Significant anticonvulsant activity has been observed also for propranolol and mexiletine—well known antiarrhythmic drugs which exert properties of stabilizing neuronal cellular membrane potential and therefore exhibit some anticonvulsant activity.[3–5] They both contain structural features which drew our attention to the chemical group of aminoalkanol derivatives.

Aminoalkanol derivatives and their anticonvulsant activity have been subject of our interest for many years, and among this group a couple drug candidates have been selected. For instance, (2,6-dimethylphenoxy)ethyl derivatives of 1,2-aminoalkanols (*e.g.*

* Corresponding author.
E-mail address: awaszkie@cm-uj.krakow.pl (A.M. Waszkielewicz).

http://dx.doi.org/10.1016/j.bmc.2016.03.006
0968-0896/© 2016 Elsevier Ltd. All rights reserved.

S-(+)-2-aminobutan-1-ol, *R*-(−)-2-aminopropan-1-ol, D,L-*trans*-2-aminocyclohexan-1-ol) have proved the highest activity in current-evoked seizures so far (Fig. 1).[6–8] It is interesting that among synthesized compounds the configuration in the aminoalkanol moiety is important—one of the enantiomers is usually more active than the other—but it also depends on the whole structure, which enantiomer will prove more potent. Within our synthetic research we have already done modification of ethyl or propyl linker between amine and phenoxyl group into ethoxyethyl in case of antidepressant-like activity, and in that case such modification proved successful.[9]

The aim of our study was to see if modification of the alkyl linker between amine and phenoxyl group into ethoxyethyl improves also anticonvulsant activity in the title group of compounds. The premise to use the same linker was common etiology and comorbidity of depression and epilepsy as well as certain similarity of stabilization of neuronal membrane potential of both anticonvulsant and antidepressant drugs.[10] Another purpose of the study was to examine whether substitution in the phenoxyl moiety stays optimal for 2,6-$(CH_3)_2$ also the case of ethoxyethyl derivatives. Therefore, we aimed to modify the most active compounds in terms of substitution in the phenyl ring in order to find optimal structures in the title group.

The studies resulted in filing of some promising compounds for a European patent.[11] Moreover, pharmacological output of the compounds resulting in probable mechanism of action, drew our attention towards preliminary safety, metabolic stability, and pharmacokinetics studies concerning the most active compounds.

2. Results and discussion

2.1. Chemistry

Chemical structures of the tested compounds are shown in Table 1. The title compounds included substituted (phenoxy)ethyl- (**1**–**6**, **12**–**18**), (phenoxy)propyl- (**7**–**11**), and [2-(phenoxy)ethoxy]ethylaminoalkanols (**19**–**30**). Substitutions in the phenyl ring constituted 2,3-dimethylphenol (**1**–**11**, **19**–**20**), 2,4-dimethylphenol (**12**–**13**), xylenol (**21**–**28**), and 2,4,6-trimethylphenol (**14**–**18**, **29**–**30**). The aminoalkanols were used the same as formerly proved optimal for anticonvulsant activity: 2-aminopropan-1-ol, 2-aminobutan-1-ol, 2- or 4-aminocyclohexan-1-ol. Moreover, for structure–activity relationship observations, 2-amino-2-methylpropan-1-ol, 2-amino-1-phenylethan-1-ol, as well as 3- or 4-piperidinol were also used. In case of activity of a racemate, enantiomers were synthesized as well. Two compounds have been achieved also as hydrochlorides (**22a**, **23a**).

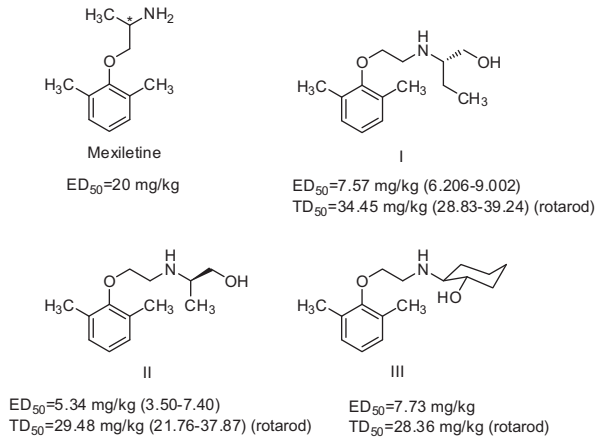

Figure 1. Reference compounds and their activity in MES, mice, *ip*.[5–8]

The synthesis of **1**–**30** (Scheme 1) was a multistage process and the final reaction constituted *N*-alkylation of appropriate aminoalkanols with use of formerly synthesized appropriate phenoxyalkyl or [2-(phenoxy)ethoxy]ethyl bromides which had been formerly prepared according to published procedures.[9,6,12] Two compounds have been characterized as hydrochlorides (**22a**, **23a**), which were obtained from base in an acetone solution of gaseous HCl.

The absolute configuration of the structure **22a** was confirmed with use of X-ray structure analysis (the crystals were obtained from a mixture of acetone and *n*-decane (1:1) by slow evaporation of the solvent at room temperature). The asymmetric unit of **22a** with the atom numbering scheme of non-hydrogen atoms is shown in Figure 2.

The crystal structure of **22a** confirms *R* configuration at carbon atom C2. The bond lengths and bond angles have typical values. The arrangement of the ether oxygen atoms (O3) and (O2) shows synclinal conformation (gauche). Furthermore, the conformation of respective pairs of atoms (O2) and (N1), (N1) and (O1) is also synclinal. The same conformation was observed in crystal structures of similar compounds *R*-2-[2-(2,6-dimethylphenoxy)ethyl] aminopropan-1-ol hydrochloride[8] and mexiletine.[13] The methyl substituents at phenoxy moiety are coplanar with benzene ring. The deviation of C14 and C15 from the benzene plane is 0.007 (5) Å and 0.050(5) Å, respectively. The carbon (C4, C5, C6, C7) and oxygen (O2) atoms of ethoxyethyl moiety lie in one plane with the rms deviation of the atoms 0.061 Å, which is almost parallel to benzene plane, with the interplanar angle 1.8(3)°.

The geometry of 2-aminopropan-1-ol moiety present in the crystal structure of **22a** molecule and *R*-2*N*-[2-(2,6-dimethylphenoxy)ethyl]aminopropan-1-ol hydrochloride was compared. The main difference is observed for the orientation of hydroxyl group. The respective torsion angle N1–C2–C1–O1 in **22a** is −76.47°, whereas in the compared structure is 45.99°.[8]

The arrangement of **22a** molecules in the crystal lattice is dominated by hydrogen bonds with chlorine anion (Table 2). Each chlorine anion interacts with two molecules forming hydrogen bond with N1–HN1 and O1–H1 of one molecule and N1–HN2 of the second one (Fig. 3). Furthermore, chlorine anion is involved in C–H interactions. The crystal structure of **22a** is also stabilized by weak C–H···O interactions.

2.2. Enantiomeric purity

The examples of the representative chromatographic traces resulted for enantiomeric forms of studied aminoalkanols derivatives (**22**, **23** and **22a**) under the optimized method conditions are presented in Figure 4. Well separated chromatographic peaks are seen, corresponding to the enantiomers of *R*,*S*-2*N*-{2-[2-(2,6-dimethylphenoxy)ethoxy]ethyl}aminopropan-1-ol (compound **21**): *R*-(−)-2*N*-{2-[2-(2,6-dimethylphenoxy)ethoxy]ethyl}aminopropan-1-ol hydrochloride (compound **22a**) and *S*-(+)-2*N*-{2-[2-(2,6-dimethylphenoxy)ethoxy]ethyl}aminopropan-1-ol (compound **23**). The studied compounds were obtained with enantiomeric excess as high as 98%.

2.3. Pharmacology

The screening results in mice are presented in Table 1. Within the title group of compounds, ethoxyethyl modification of compound II—compound **22a** exhibits similar activity of the reference compound. ED_{50} in MES, mice, *ip* is observed 5.34 (3.50–7.40) for hydrochloride of compound II[8] and 12.92 (8.49–19.01) for compound **22a** (Table 3). It should be noticed that the confidence intervals do not cover which suggests that the compounds may have different pharmacological profiles. However, at this point it seems that the difference in activity of the enantiomers is slight.

Table 1
Structures and screening results of compounds **1–30** (mice, *ip*)

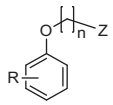

Comp. **1-18**

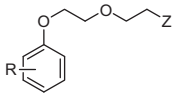

Comp. **19-30**

Compound	R	*n*	Z	Configuration	Dose (mg/kg)	Time (h)									
						MES[a]				ScMet[a]		TOX[b]			
						0.25	0.5	1.0	4.0	0.5	4.0	0.25	0.5	1.0	4.0
1	2,3-$(CH_3)_2$	2	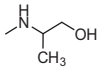	*R,S*	30 100 300		0/1 **3/3**		0/1 0/3	0/1 0/1	0/1 0/1		0/4 7/8 4/4		0/2 0/4
2			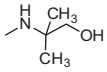	—	30 100 300		0/1 **3/3**		0/1 0/3	0/1 0/1	0/1 0/1		0/4 7/8 4/4		0/2 0/4
3			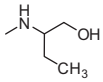	*R,S*	30 100 300		0/1 **3/3**		0/1 0/3	0/1 0/1	0/1 0/1		0/4 8/8 4/4		0/2 0/4
4			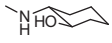	D,L-*trans*	100	**4/4**	**4/4**	**4/4**	0/4			4/4	4/4	4/4	0/4
5			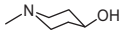	—											
6			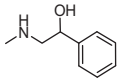	*R,S*	30 100 300		0/1 0/3 0/1		0/1 0/3 0/1	1/5 0/1 0/1	0/1 0/1 0/1		0/4 4/8 3/4		0/2 1/4 0/2
7		3	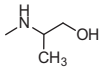	*R,S*	30 100 300		0/1 **3/3**		0/1 0/3	0/1 0/1	0/1 0/1		0/4 8/8 4/4		0/2 0/4
8			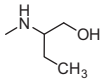	*R,S*	30 100 300		0/1 **3/3**		0/1 0/3	0/1 0/1	0/1 0/1		0/4 8/8 4/4		0/2 0/4
9				—	30 100	**3/4** **4/4**	**3/4** **4/4**	0/4 **4/4**	0/4 0/4			0/4 3/4	0/4 3/4	0/4 0/4	0/4 0/4
10			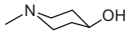	—	100	**4/4**	**4/4**	**1/4**	0/4			3/4	1/4	0/4	0/4
11			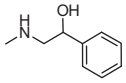	*R,S*	30 100 300	0/3	0/1 0/3 **1/1**	0/3	0/1 0/3 0/1	0/1 0/1 0/1	0/1 0/1 0/1	3/3	1/4 6/8 4/4	3/3	1/2 3/4 2/2
12	2,4-$(CH_3)_2$	2	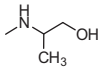	*R,S*											
13			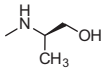	*R*											
14	2,4,6-$(CH_3)_3$		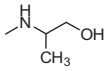	*R,S*	30 100 300		0/1 **3/3**		0/1 0/3	0/1 0/1	0/1 0/1		0/4 8/8 4/4(1)		0/2 0/4
15			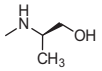	*R*	3 10 30 100 300		0/4 0/4 **1/1** **3/3**		0/1 0/3	0/1 0/1	0/1 0/1		0/4 0/4 0/4 8/8 4/4(1)		0/2 0/4
16			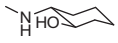	D,L-*trans*	3 10 30 100 300		0/4 **1/4** **1/1**		0/1 0/1	0/1 0/1	0/1 0/1		0/4 1/4 0/4 8/8(6) 4/4(4)		0/2 0/2 1/1
17			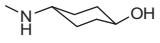	*trans*	30 100 300		0/1 **2/2**		0/1 0/3	0/1 0/1	0/1		0/4 2/8(1) 4/4(1)		0/2 0/3

(*continued on next page*)

Table 1 (*continued*)

Compound	R	*n*	Z	Configuration	Dose (mg/kg)	Time (h)									
						MES[a]				ScMet[a]		TOX[b]			
						0.25	0.5	1.0	4.0	0.5	4.0	0.25	0.5	1.0	4.0
18			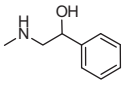	*R,S*	30 100 300		0/1 **3/3** **1/1**		0/1 0/3 **1/1**(1)	0/1 0/1 0/1			0/4 0/8 3/4		0/2 0/4 0/2
19	2,3-$(CH_3)_2$	—	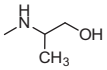	*R,S*	30 100 300		0/1		0/1 0/1	0/1	0/1 0/1		0/4 8/8(7) 4/4(3)		0/2 0/1 0/1
20			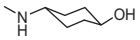	*trans*											
21	2,6-$(CH_3)_2$	—	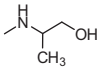	*R,S*	30 100 300		0/1		0/1 0/1	0/1	0/1 0/1		0/4 8/8 4/4		0/2 0/1 0/1
22			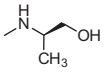	*R*	3 10 30 100 300		0/4 **1/4** **1/1**		0/1	0/1	0/1		0/4 0/4 0/4 8/8(8) 4/4(4)		0/2
22a			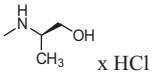	*R*	3 10 30 100 300		0/4 **1/4** **1/1**		0/1	0/1	0/1		0/4 0/4 0/4 8/8(8) 4/4(4)		0/2
23			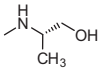	*S*	3 10 30 100 300		0/4 **2/4** **1/1**		0/1	0/1	0/1		0/4 0/4 1/4 8/8(8) 4/4(4)		0/2
23a			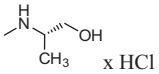	*S*	3 10 30 100 300		0/4 0/4 **1/1**		0/1	0/1	0/1		0/4 0/4 0/4 8/8(8) 4/4(4)		0/2
24			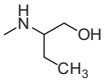	*R,S*	30 100 300		0/1 **1/1**		0/1 0/1	0/1 0/1	0/1 0/1		0/4 8/8(7) 4/4(1)		0/2 0/2
25			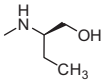	*R*	3 10 30 100 300		0/4 0/4 **1/1**		0/4 0/4 0/1 0/1	0/1	0/1		0/4 0/4 0/4 7/8(7) 4/4(4)		0/4 0/4 0/2 0/1
26			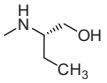	*S*	3 10 30 100 300		0/4 0/4 **1/1**		0/1	0/1	0/1		0/4 0/4 0/4 8/8(8) 4/4(4)		0/2
27				D,L-*trans*	30 100 300		0/1 **3/3**		0/1 0/3	0/1 0/1	0/1 0/1		0/4 0/8 4/4(4)		0/2 0/4
28			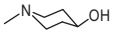	-	30 100 300		0/1		0/1 0/1	0/1	0/1 0/1		0/4 7/8(6) 4/4(4)		0/2 0/2
29	2,4,6-$(CH_3)_3$	—	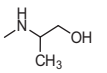	*R,S*	30 100 300		0/1 **3/3**		0/1 **1/3**	0/1 0/1	0/1 0/1		0/4 4/8 4/4(4)		0/2 0/4
30				D,L-*trans*											

[a] No. of animals protected/no. of animals tested.
[b] No. of animals exhibiting neurotoxicity/no. of animals tested in rotarod, (deaths).

The ED_{50} was also determined for compound **23** and it can be compared to the *S* enantiomer of compound II, taking into account the whole confidence intervals of the active dose. The ethoxyethyl derivative exhibits ED_{50} (MES, mice, *ip*) 11.3 (9.39–13.3) mg/kg b.w. (Table 3) while its lead ED_{50} is 8.59 (7.23–10.03) mg/kg b.w.[8] Moreover, the compound is active after intraperitoneal administration to rats (Table 4). Its hydrochloride shows the same potency in the assay.

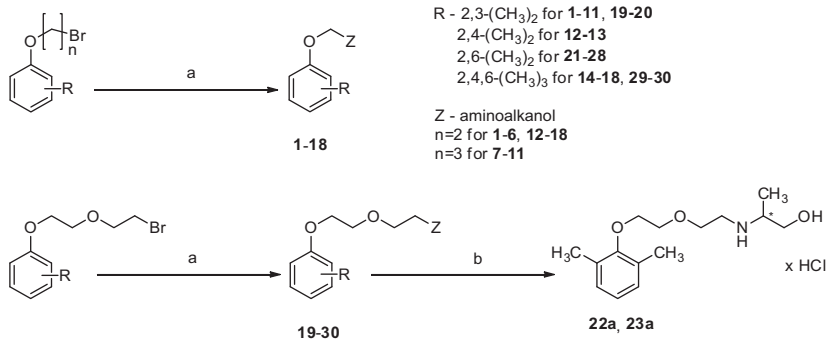

Scheme 1. Synthetic routes to final compounds. Reagents: (a) *Z*-aminoalkanol, K_2CO_3/toluene or acetone (TEBA); (b) gaseous HCl/acetone.

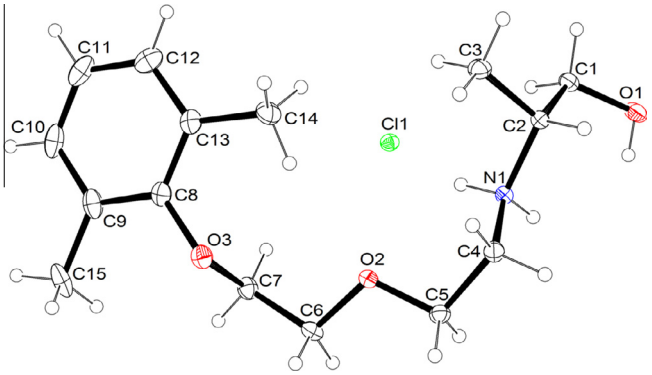

Figure 2. The molecular structure of **22a** showing the atom numbering scheme. Displacement ellipsoids are drawn at the 50% probability level.

Table 2
Intermolecular interaction for **22a**

D–H···A	H···A (Å)	D···A (Å)	D–H–A (°)	Symmetry code
N1–HN2···Cl1	2.34(5)	3.232(2)	160(3)	
N1–HN1···Cl1	2.21(4)	3.127(2)	178(3)	$-x+1, y-1/2, -z+2$
O1–H1···Cl1	2.32(5)	3.136(2)	174(4)	$-x+1, y-1/2, -z+2$
C1–H1A···Cl1	2.92	3.743(3)	143.8	
C3–H3C···Cl1	2.85	3.773(3)	161.8	$-x, y-1/2, -z+2$
C4–H4B···Cl1	2.77	3.640(3)	149.5	$x, y-1, z$
C6–H6B···O1	2.60	3.175(3)	117.9	$-x+1, y+1/2, -z+2$

In terms of the ethoxyethyl analog of compound III—compound **7**, its activity was not strong enough to determine ED_{50}. Anticonvulsant properties are observed in rats after 1 h of oral administration, which may suggest activity of its metabolite (Table 4).

Since many registered drugs were developed with use of MES test screening, and efficacy of these drugs is not satisfactory, another screening test has been introduced in the Antiepileptic Drug Development program, *i.e.* the 6 Hz test (for epileptogenesis, psychomotor seizures, etc.).[14] Compounds **4**–**5**, **9**–**10**, **12**, **19**, **22**–**23a**, and **30** were subject to such screening at various doses and their activity was observed in time (Table 5). Comparing these results, compounds **4**, **9**–**10**, **19**, **23**, **23a** were tested in both MES and 6 Hz tests and TOX (Tables 1 and 5).

Considering activity of the most active compounds **22** and **23**, both of them could be compared in 6 Hz test (Table 5)—compound **22** exhibits interesting activity at 50 mg/kg for 1 h after administration and after 4 h, which presumes activity of a metabolite as well. For comparison, compound **23** tested at 40 mg/kg exhibits similar activity until 4 h after administration. Results of the hydrochloride **23a** are consistent with efficacy of the base **23**.

The interesting pharmacological results of compound **22** drew our attention to probability of activity of either the compound itself or its metabolite, since the activity in the 6 Hz test was observed until 1 h after administration. Then, after 4 h some activity appeared again, which suggests positive effects of a metabolite. Similar effect is observed for compounds **5** and **23a**.

Compounds **22a** and **23** have been also evaluated in pilocarpine-induced status epilepticus and the results are presented in Table 6. On one hand, deaths are observed at very high doses short after administration of relatively (for rats) high doses of the tested compound. However, status epilepticus is itself risk of life, therefore, it is often observed in results of this test that animals die, and in the case of **22a** at a dose of 400 mg/kg no animal died.

Within the Anticonvulsant Drug Development program ADD,[15] due to promising anticonvulsant activity of **22a**, the compound was advanced to evaluation of analgesic activity in neurogenic pain in the formalin test (mice, *ip*). The premise for such considerations

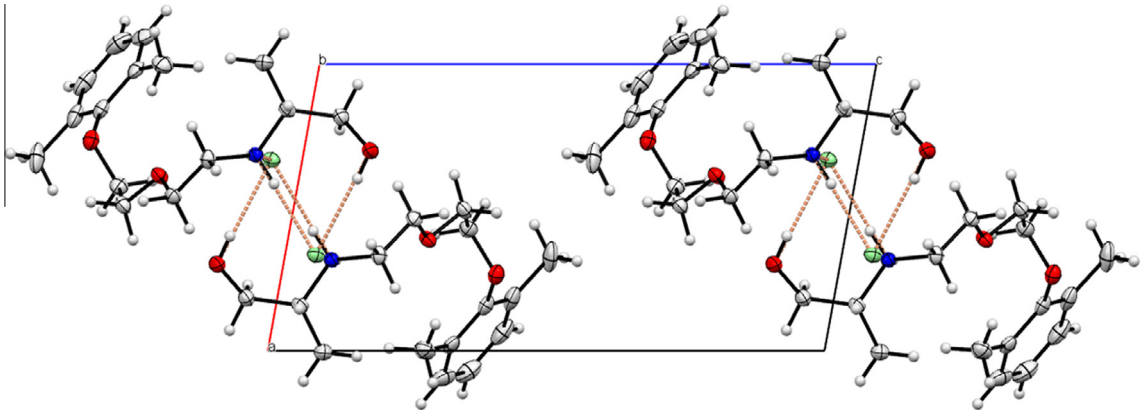

Figure 3. Packing of molecules in the unit cell of the crystalline **22a** projected along [0 1 0] direction. Dashed lines indicate hydrogen bonds.

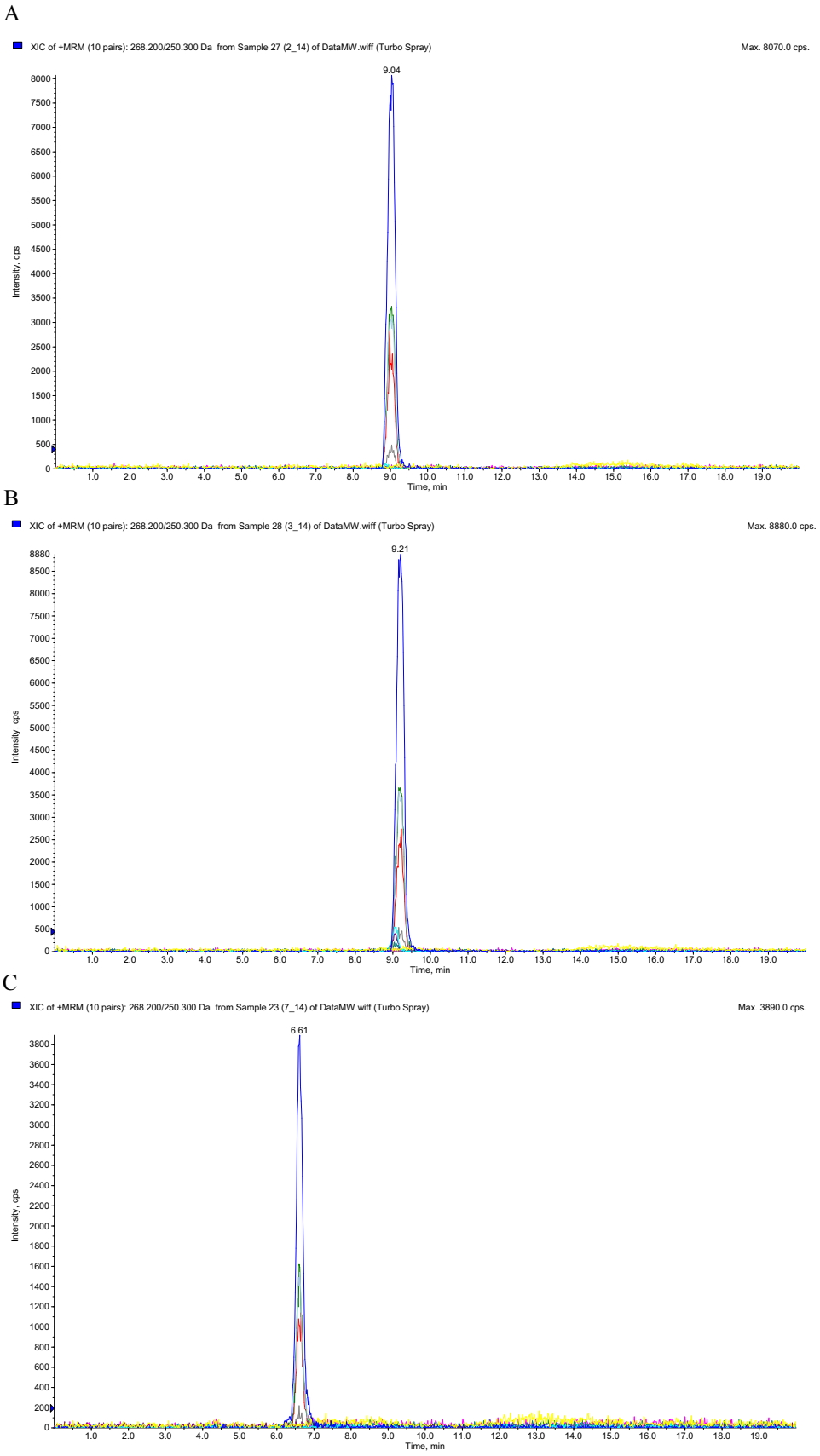

Figure 4. The mass chromatograms of **22** (A), **23** (B) and **22a** (C).

Table 3
ED_{50} and TD_{50} in mice, *ip* at 0.25 h

Compound	MES ED_{50} (mg/kg) (confidence interval)	ScMet ED_{50} (mg/kg)	TD_{50} (mg/kg) (confidence interval)
22a	12.92 (8.49–19.01)	>45.0[D]	33.26 (31.33–35.71)
23	11.3 (9.39–13.3)	>43.0	39.24 (32.27–43.72)
II[8]	5.34 (3.50–7.40)	>50	29.48 (21.76–37.87)

[D] Death.

are, as formerly stated—stabilization of neuronal membrane potential exhibited by many anticonvulsants. The results of the test are presented in Figure 5 and Table 7. Within the acute phase of the test (10 min after injection of formaldehyde), the analgesic activity is significant. Activity in the inflammatory phase (the remaining time of the 40-min test) is not significant, however, some effect is visible.

Due to the above considerations, compounds **22a** and **23a** were subject to search for mechanism of action with use of radioligand binding studies. Therefore, standard high throughput profile (Cerep, France) was performed for them. In order to extract maximum information regarding safety *e.g.* at intravenous administration, a high concentration 10^{-5} M was chosen as preliminary. The results are presented in Table 8, and they indicate that the compounds look as quite "clean pharmacophores" since the strongest binding is observed only for σ, 5-HT transporter, 5-HT_{2B}, 5-HT_{1A}. Nevertheless, for the less interesting **23a**, some binding is observed for sodium channels, norepinephrine transporter, D_3, κ, NK_1. Therefore, due to more promising results of **22a**, hERG binding was also determined

Table 5
Anticonvulsant activity of selected compounds in the 6 Hz and TOX tests (mice, *ip*)

Compound	Test	Dose (mg/kg)	Time[a] (h)				
			0.25	0.5	1.0	2.0	4.0
4	6 Hz[a]	50	**2/4**	0/4	0/4	0/4	0/4
	TOX[b]	50	**1/4**	0/4	0/4	0/4	0/4
5	6 Hz	100	**3/4**	**2/4**	0/4	0/4	**1/4**
	TOX	100	**1/4**	0/4	0/4	0/4	0/4
9	6 Hz	100	**2/4**	**2/4**	**2/4**	0/4	0/4
	TOX	100	**2/4**	**2/4**	**2/4**	0/4	0/4
10	6 Hz	100	**3/4**	**3/4**	**2/4**	0/4	0/4
	TOX	100	**2/4**	**3/4**	**1/4**	0/4	0/4
12	6 Hz	100	**2/4**	0/4	0/4	0/4	0/4
	TOX	100	**2/4**	**2/4**	0/4	0/4	0/4
19	6-Hz	100	**4/4**	**3/4**	**4/4**	0/4	0/4
	TOX	100	**4/4**	**3/4**	0/4	0/4	0/4
22	6-Hz	50	**3/4**	**4/4**	**2/4**	0/4	**2/4**
	TOX	50	**3/4**	**3/4**	0/4	0/4	0/4
23	6-Hz	20	0/4	0/4	0/4	0/4	0/4
	6-Hz	40	**3/4**	**4/4**	**2/4**	**1/4**	**1/4**
	TOX	20	0/4	0/4	0/4	0/4	0/4
	TOX	40	**4/4**	**2/4**	0/4	0/4	0/4
23a	6-Hz	30	**2/4**	**2/4**	0/4	0/4	**2/4**
	TOX	30	0/4	0/4	0/4	0/4	0/4
30	6-Hz	50	**2/4**	**2/4**	0/4	0/4	0/4
	TOX	50	**3/4**	0/4	0/4	0/4	0/4

[a] No. of animals protected/no. of animals tested.
[b] No. of animals exhibiting neurotoxicity/no. of animals tested in rotarod, '—' compound was not tested in these conditions.

Table 4
Anticonvulsant activity of selected compounds in the MES and TOX tests (rats)

Compound	Route of administration	Test	Dose (mg/kg)	Time[a] (h)				
				0.25	0.5	1.0	2.0	4.0
9	*ip*	MES[a]	30	**3/4**	**3/4**	0/4	**1/4**	0/4
		TOX[b]	30	0/4	0/4	0/4	0/4	0/4
	p.o.	MES	30	0/4	0/4	0/4	0/4	0/4
		TOX	30	0/4	0/4	0/4	0/4	0/4
10	*ip*	MES	30	**3/4**	**3/4**	**1/4**	0/4	0/4
		TOX	30	0/4	0/4	0/4	0/4	0/4
	ip	MES	30	**3/4**	**3/4**	**1/4**	0/4	0/4
		TOX	30	0/4	0/4	0/4	0/4	0/4
	p.o.	MES	30	0/4	0/4	0/4	0/4	0/4
		TOX	30	0/4	0/4	0/4	0/4	0/4
14	*p.o.*	MES	30	0/4	**1/4**	0/4	0/4	0/4
		TOX	30	0/4	0/4	0/4	0/4	0/4
16	*p.o.*	MES	30	**1/4**	0/4	0/4	0/4	**1/4**
		TOX	30	0/4	0/4	0/4	0/4	0/4
17	*p.o.*	MES	30	0/4	0/4	0/4	0/4	0/4
		TOX	30	0/4	0/4	0/4	0/4	0/4
18	*p.o.*	MES	30	0/4	**2/4**	0/4	**2/4**	2/4
		TOX	30	0/4	0/4	0/4	0/4	0/4
23	*ip*	MES	30	**4/4**	**4/4**	**3/4**	0/4	0/4
		TOX	30	0/4	0/4	0/4	0/4	0/4
	p.o.	MES	30	0/4	0/4	0/4	0/4	0/4
		TOX	30	0/4	0/4	0/4	0/4	0/4
23a	*ip*	MES	30	**4/4**	**4/4**	**3/4**	0/4	0/4
		TOX	30	0/4	0/4	0/4	0/4	0/4
	p.o.	MES	30	0/4	0/4	0/4	0/4	0/4
		TOX	30	0/4	0/4	0/4	0/4	0/4
26	*p.o.*	MES	30	0/4	0/4	0/4	0/4	0/4
		TOX	30	0/4	0/4	0/4	0/4	0/4
27	*p.o.*	MES	30	0/4	0/4	**1/4**	0/4	0/4
		TOX	30	0/4	0/4	0/4	0/4	0/4

[a] No. of animals protected/no. of animals tested.
[b] No. of animals exhibiting neurotoxicity /no. of animals tested in rotarod, '—' compound was not tested in these conditions.

Table 6
Activity in pilocarpine-induced status epilepticus test (rats, *ip*)

Compound	Dose (mg/kg)	Time[a] (h)					Dose (mg/kg b.w.)	Time[a] (h)	Effect[c]	Average weight change (g) ± SEM[b]	
		0.25 h	0.5 h	1.0 h	2.0 h	4.0 h					
22a	30	0/2	0/2	0/2	0/2	0/2	65	0	0/8[a]		
	100	**1/2**[D]	0/1	0/1	0/1	0/1	400	0.5	6/8[S]	17.5 ± 5.2	25.0 ± 5.0
23	30	**1/2**[A]	0/2	0/2	0/2	0/2					
	100	**2/2**[D]									

[a] Post first stage 3 seizure.
[b] Weight change 24 h post first stage 3 seizure.
[c] No. of animals protected/no. of animals tested.
[S] Sedation.
[A] Ataxia.
[D] Death.

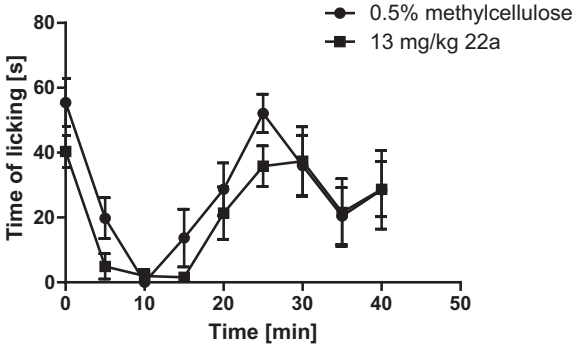

Figure 5. Analgesic properties of **22a** in the formalin test, mice, *ip*.

Table 7
Results of formalin test for compound **22a** (mice, *ip*)

Dose (mg/kg b.w.)	Phase	Area under the curve (AUC)				
		Control	**22a**	% of control	SEM	*P*
13.0	Acute	237.47	130.39	54.9	11.52	<0.05
13.0	Inflammatory	819.6	665.07	81.14	10.43	>0.05

at 10^{-4} M for verification of preliminary cardiac safety, which is obligatory for all drug candidates (Table 8).

2.4. Mutagenic or antimutagenic activity

Compounds **21**, **22a**, **23**, and **25**–**30** have been also subject to preliminary evaluation of mutagenic properties in the *Vibrio harveyi* test and the results are presented in Table 9. It is clearly visible, that not only the most interesting compounds **22a** and **23**, but all evaluated samples, are not mutagenic. Due to accessibility of the test, additionally antimutagenic properties have been tested. The results are presented in Tables 10 and 11. The latter one serves as a conclusion of such properties of the tested compounds—none of them is mutagenic. Compounds **21**, **27**, and **29** exhibit significant although unexpected antimutagenic potential which could be further explored.

2.5. Metabolic stability

Compounds **22a** and **23** were chosen for further investigation of metabolic stability with use of mice liver microsomes, in order to determine which compound of either pair **22a** or **23** or their metabolites are responsible for long lasting activity in rodents. Moreover, one very similar but inactive compound was added to the assay—compound **29** (racemic 4-methyl derivative of **22a** and **23**) for information regarding influence of metabolism on the activity of the compounds. The results are presented in Table 12.

According to them, compounds **22a**, **23** and **29** exhibited moderate in vitro metabolic stability. Noteworthy, compound **29** being inactive in former in vivo studies, demonstrated Cl_{int} values lying in the lower limit of the medium category range (13 μL/mg/min). On the other hand, active compounds **22a** and **23**, as enantiomers were characterized with Cl_{int} values lying at the border between medium and high intrinsic clearance values (47 μL/mg/min). Thus, it is probable that metabolites of compounds **22a** and **23** may contribute to the previously observed in vivo activity of parent compounds. Moreover, since **29** is racemic 4-methyl derivative of **22**, it can be deduced that the presence of methyl moiety in position 4 probably diminishes pharmacological activity of the compound and inhibits its metabolism.

2.6. Pharmacokinetic profile

The results of the microsomal assay became premises to evaluation of pharmacokinetic profile of the most promising compound **22a**, after its intravenous (1 mg/kg), intragastric (12.92 mg/kg) and intraperitoneal (12.92 mg/kg) administration in mice. The concentration of target compound in plasma was quantified using LC/ESI-MS/MS system, and the method was thoroughly validated. The mean plasma concentrations versus time profiles are depicted in Figure 6, whereas the pharmacokinetic parameters are given in Table 13.

After the intravenous, intragastric or intraperitoneal administration of the studied compound in mice the terminal half-lives were rather short, 51.5 min, 29.1 min, and 77.2 min, respectively, with relatively rapid elimination of the molecule from the body. The pharmacokinetic results indicate that the absorption of **22a** was rapid, with the peak concentration occurring at 5 min after an intragastric or intraperitoneal administration of target compound, and with maximum concentration found to be 950 ng/mL or 1190 ng/mL, respectively. Unfortunately, the absolute bioavailability estimated based on the $AUC_{0\rightarrow\infty}$ calculated from zero time to infinity was very low, and yielded only the values of 2.98% for intragastric or 6.78% for intraperitoneal administration. The main reason of the low bioavailability of the studied compound might be on one hand meaningful metabolism by the liver, and on the other hand, possible poorly absorption by intestine or its interaction with drug transporters. It is worth noting that the target compound has high binding affinity to mice brain (Fig. 7 and Tables 14 and 15).

3. Conclusions

The presented research resulted in **30** new compounds, among which new active structures have been found. Additionally, for compound **22a**, absolute configuration has been determined with

Table 8
Receptor binding results for **22a** and **23a** at 10^{-5} M concentration

Receptor	Mean % inhibition of control specific binding[a]		Study conditions			Reference data	
	22a	**23a**	Origin of receptor	Radioligand	Radioligand type	Compound	IC_{50} [M]
A_1	−32.2	−6.9	Human recombinant CHO cells	[^{3}H]DPCPX	Antagonist	DPCPX	$5.0 * 10^{-10}$
A_{2A}	−0.8	−4.0	Human recombinant HEK−293 cells	[^{3}H]CGS 21680	Agonist	NECA	$3.7 * 10^{-8}$
A_3	−1.8	3.0	Human recombinant HEK-293 cells	[^{125}I]ABMECA	Agonist	IB-MECA	$6.0 * 10^{-10}$
α_1	32.3	28.3	Rat cerebral cortex	[^{3}H]prazosin	Antagonist	Prazosin	$2.5 * 10^{-10}$
α_2	42.8	35.5	Rat cerebral cortex	[^{3}H]RX 821002	Antagonist	Yohimbine	$9.6 * 10^{-8}$
β_1	4.8	11.1	Human recombinant HEK-293 cells	[^{3}H](−)CGP12177	Agonist	Atenolol	$2.1 * 10^{-7}$
β_2	2.0	5.7	Human recombinant CHO cells	[^{3}H](−)CGP12177	Agonist	ICI 118551	$7.4 * 10^{-10}$
AT_1	−27.4	−28.9	Human recombinant HEK-293 cells	[^{125}I] [Sar^1,Ile^8]-ATII	Antagonist	Saralasin	$4.0 * 10^{-10}$
AT_2	6.4	11.7	Human recombinant HEK-293 cells	[^{125}I]CGP42112A	Agonist	Angiotensin-II	$8.0 * 10^{-11}$
BZD (central)	−11.0	−22.4	Rat cerebral cortex	[^{3}H]flunitrazepam	Agonist	Diazepam	$6.8 * 10^{-9}$
BZD (peripheral)	−3.9	−6.7	Rat heart	[^{3}H]PK 11195	Antagonist	PK 11195	$1.6 * 10^{-9}$
BB (non-selective)	−1.4	−5.4	Rat cerebral cortex	[^{125}I][Tyr^4]bombesin	Agonist	Bombesin	$3.4 * 10^{-10}$
B_2	−3.9	1.6	Human recombinant CHO cells	[^{3}H]bradykinin	Agonist	NPC 567	$1.4 * 10^{-8}$
CGRP	−7.5	−7.4	Human recombinant CHO cells	[^{125}I]hCGRPα	Agonist	hCGRPalpha	$3.2 * 10^{-11}$
CB_1	12.6	11.1	Human recombinant CHO cells	[^{3}H]CP 55940	Agonist	CP 55940	$9.0 * 10^{-10}$
CCK_1 (CCK_A)	−3.6	2.2	Human recombinant CHO cells	[^{125}I]CCK-8s	Agonist	CCK-8s	$1.3 * 10^{-10}$
CCK_2 (CCK_B)	−16.4	−32.0	Human recombinant CHO cells	[^{125}I]CCK-8s	Agonist	CCK-8s	$1.2 * 10^{-10}$
D_1	12.4	16.2	Human recombinant CHO cells	[^{3}H]SCH23390	Antagonist	SCH 23390	$3.1 * 10\_^{10}$
D_{2S}	12.0	14.7	Human recombinant HEK-293 cells	[^{3}H]methylspiperone	Antagonist	(+)butaclamol	$1.1 * 10^{-9}$
D_3	44.1	**57.4**	Human recombinant CHO cells	[^{3}H]methylspiperone	Antagonist	(+)butaclamol	$1.6 * 10^{-9}$
$D_{4.4}$	40.9	35.8	Human recombinant CHO cells	[^{3}H]methylspiperone	Antagonist	Clozapine	$4.1 * 10^{-8}$
D_5	10.1	5.2	Human recombinant GH4 cells	[^{3}H]SCH23390	Antagonist	SCH 23390	$5.6 * 10^{-10}$
ET_A	−3.4	−4.4	Human recombinant CHO cells	[^{125}I]endothelin-1	Agonist	Endothelin-1	$2.3 * 10^{-11}$
ET_B	−15.6	−24.2	Human recombinant CHO cells	[^{125}I]endothelin-1	Agonist	Endothelin-3	$6.3 * 10^{-12}$
GABA (non-selective)	0.8	17.7	Rat cerebral cortex	[^{3}H]GABA	Agonist	GABA	$2.1 * 10^{-8}$
GAL_1	−0.7	−0.4	Human recombinant HEK-293 cells	[^{125}I]galanin	Agonist	Galanin	$7.9 * 10^{-11}$
GAL_2	−16.5	−11.1	Human recombinant CHO cells	[^{125}I]galanin	Agonist	Galanin	$2.6 * 10^{-9}$
PDGF	−12.5	−5.6	Balb/c 3T3 cells	[^{125}I]PDGF BB	Agonist	PDGF BB	$4.7 * 10^{-11}$
CXCR2 (IL-8B)	2.9	2.7	Human recombinant HEK-293 cells	[^{125}I]IL-8	Agonist	IL-8	$5.1 * 10^{-11}$
CCR1	−11.2	−14.2	Human recombinant HEK-293 cells	[^{125}I]MIP-1α	Agonist	MIP-1alpha	$2.1 * 10^{-11}$
TNF-α	5.1	4.6	U-937 cells	[^{125}I]TNF-α	Agonist	TNF-alpha	$9.9 * 10^{-11}$
H_1	22.7	14.1	Human recombinant HEK-293 cells	[^{3}H]pyrilamine	Antagonist	Pyrilamine	$1.4 * 10^{-9}$
H_2	0.6	17.1	Human recombinant CHO cells	[^{125}I]APT	Antagonist	Cimetidine	$1.0 * 10^{-6}$
MC_4	5.3	9.0	Human recombinant CHO cells	[^{125}I]NDP-α-MSH	Agonist	NDP-alpha-MSH	$1.5 * 10^{-10}$
MT_1 (ML_{1A})	−12.2	−7.5	Human recombinant CHO cells	[^{125}I]2-iodomelatonin	Agonist	Melatonin	$1.1 * 10^{-10}$
M_1	6.0	22.8	Human recombinant CHO cells	[^{3}H]pirenzepine	Antagonist	Pirenzepine	$2.1 * 10^{-8}$
M_2	20.8	37.2	Human recombinant CHO cells	[^{3}H]AF-DX384	Antagonist	Methoctramine	$2.2 * 10^{-8}$
M_3	8.5	4.4	Human recombinant CHO cells	[^{3}H]4-DAMP	Antagonist	4-DAMP	$4.1 * 10^{-10}$
M_4	11.2	15.7	Human recombinant CHO cells	[^{3}H]4-DAMP	Antagonist	4-DAMP	$4.9 * 10^{-10}$
M_5	8.6	5.7	Human recombinant CHO cells	[^{3}H]4-DAMP	Antagonist	4-DAMP	$3.2 * 10^{-10}$
NK_1	17.3	**51.7**	U-373MG cells (endogenous)	[^{125}I]BH-SP	Agonist	[Sar9,Met(O2)11]-SP	$1.1 * 10^{-10}$
NK_2	2.2	41.2	Human recombinant CHO cells	[^{125}I]NKA	Agonist	[Nleu10]-NKA (4–10)	$3.5 * 10^{-9}$
NK_3	8.0	15.0	Human recombinant CHO cells	[^{3}H]SR142801	Antagonist	SB 222200	$6.7 * 10^{-9}$
Y_1	−34.5	−29.6	SK-N-MC cells (endogenous)	[^{125}I]peptideYY	Agonist	NPY	$2.1 * 10^{-10}$
Y_2	−5.1	−14.5	KAN-TS cells	[^{125}I]peptideYY	Agonist	NPY	$2.8 * 10^{-11}$
NTS_1 (NT_1)	−4.2	−10.5	Human recombinant CHO cells	[^{125}I]Tyr3-neurotensin	Agonist	Neurotensin	$4.9 * 10^{-10}$
δ_2 (DOP)	−1.7	−2.2	Human recombinant CHO cells	[^{3}H]DADLE	Agonist	DPDPE	$1.3 * 10^{-9}$
κ (KOP)	29.3	**54.0**	Rat recombinant CHO cells	[^{3}H]U 69593	Agonist	U 50488	$6.4 * 10^{-10}$
μ (MOP)	23.6	40.2	Human recombinant HEK-293 cells	[^{3}H]DAMGO	Agonist	DAMGO	$4.3 * 10^{-10}$
NOP (ORL1)	1.5	0.2	Human recombinant HEK-293 cells	[^{3}H]nociceptin	Agonist	Nociceptin	$1.3 * 10^{-9}$
PAC_1 (PACAP)	−38.2	−12.1	Human recombinant CHO cells	[^{125}I]PACAP1-27	Agonist	PACAP1-38	$4.0 * 10^{-11}$
$PPAR_\gamma$	−12.7	−26.0	Human recombinant (*E. coli*)	[^{3}H]rosiglitazone	Agonist	Rosiglitazone	$1.0 * 10^{-8}$
PCP	9.6	5.8	Rat cerebral cortex	[^{3}H]TCP	Antagonist	MK 801	$4.6 * 10^{-9}$
EP_2	3.4	11.2	Human recombinant HEK-293 cells	[^{3}H]PGE_2	Agonist	PGE2	$2.6 * 10^{-9}$

(*continued on next page*)

Table 8 (*continued*)

Receptor	Mean % inhibition of control specific binding[a]		Study conditions			Reference data	
	22a	**23a**	Origin of receptor	Radioligand	Radioligand type	Compound	IC_{50} [M]
EP_4	14.9	3.0	Human recombinant HEK-293 cells	[^{3}H]PGE2	Agonist		
IP (PGI_2)	−11.5	−6.0	Human recombinant HEK-293 cells	[^{3}H]iloprost	Agonist	Iloprost	$1.0 * 10^{-8}$
P2X	3.5	4.8	Rat urinary bladder	[^{3}H]α,β-MeATP	Agonist	alpha,beta-MeATP	$1.9 * 10^{-9}$
P2Y	9.4	9.4	Rat cerebral cortex	[^{35}S]dATPαS	Agonist	dATPalpha S	$2.9 * 10^{-8}$
5-HT_{1A}	**70.6**	**63.9**	Human recombinant HEK-293 cells	[^{3}H]8-OHDPAT	Agonist	8-OH-DPAT	$5.3 * 10^{-10}$
5-HT_{1B}	−1.8	16.5	Rat cerebral cortex	[^{125}I]CYP (+30 μM isoproterenol)	Antagonist	Serotonin	$4.9 * 10^{-9}$
5-HT_{2A}	22.6	32.1	Human recombinant HEK-293 cells	[^{3}H]ketanserin	Antagonist	Ketanserin	$3.5 * 10^{-10}$
5-HT_{2B}	**89.4**	**78.8**	Human recombinant CHO cells	[^{125}I](±)DOI	Agonist	(±)DOI	$2.5 * 10^{-9}$
5-HT_{2C}	34.7	47.4	Human recombinant HEK-293 cells	[^{3}H]mesulergine	Antagonist	RS 102221	$1.5 * 10^{-9}$
5-HT_3	29.4	12.3	Human recombinant CHO cells	[^{3}H]BRL43694	Antagonist	MDL 72222	$6.9 * 10^{-9}$
5-HT_{5A}	4.2	10.7	Human recombinant HEK-293 cells	[^{3}H]LSD	Agonist	Serotonin	$1.8 * 10^{-7}$
5-HT_6	6.7	15.4	Human recombinant CHO cells	[^{3}H]LSD	Agonist	Serotonin	$1.2 * 10^{-7}$
5-HT_7	24.5	24.6	Human recombinant CHO cells	[^{3}H]LSD	Agonist	Serotonin	$2.5 * 10^{-10}$
σ (non-selective)	**92.9**	**95.6**	Jurkat cells (endogenous)	[^{3}H]DTG	Agonist	Haloperidol	$1.7 * 10^{-8}$
sst (non-selective)	−5.5	−2.0	AtT-20 cells	[^{125}I]Tyr11-somatostatin-14	Agonist	Somatostatin-14	$7.4 * 10^{-11}$
GR	31.3	8.3	IM-9 cells (cytosol)	[^{3}H]dexamethasone	Agonist	Dexamethasone	$3.8 * 10^{-9}$
$VPAC_1$ (VIP_1)	−11.9	−17.8	Human recombinant CHO cells	[^{125}I]VIP	Agonist	VIP	$1.1 * 10^{-10}$
V_{1a}	−3.2	−0.8	Human recombinant CHO cells	[^{3}H]AVP	Agonist	[d(CH2)51,Tyr(Me)2]-AVP	$9.9 * 10^{-10}$
Ca^{2+} channel (L, verapamil site)	43.6	65.9	Rat cerebral cortex	[^{3}H]D888	Antagonist	D 600	$1.5 * 10^{-8}$
K_V channel	−20.9	−15.9	Rat cerebral cortex	[^{125}I]α-dendrotoxin	Antagonist	Alpha-dendrotoxin	$5.7 * 10^{-10}$
SK_{Ca} channel	−11.1	−0.9	Rat cerebral cortex	[^{125}I]apamin	Antagonist	Apamin	$1.6 * 10^{-11}$
Na^+ channel (site 2)	**54.9**	**79.0**	Rat cerebral cortex	[^{3}H]batrachotoxinin	Antagonist	Veratridine	$4.0 * 10^{-6}$
Cl^- channel (GABA-gated)	−7.6	4.6	Rat cerebral cortex	[^{35}S]TBPS	Antagonist	Picrotoxinin	$7.7 * 10^{-8}$
Norepinephrine transporter (h)	**52.6**	34.5	Human recombinant CHO cells	[^{3}H]nisoxetine	Antagonist	Protriptyline	$2.8 * 10^{-9}$
Dopamine transporter	24.5	16.2	Human recombinant CHO cells	[^{3}H]BTCP	Antagonist	BTCP	$2.8 * 10^{-9}$
5-HT transporter	**96.5**	**91.4**	Human recombinant CHO cells	[^{3}H]imipramine	Antagonist	Imipramine	$8.8 * 10^{-10}$
hERG (at 10^{-4} M)	**3.6**	–	Human recombinant HEK-293 cells	[^{3}H]astemizole	Antagonist		

The bold values show >50% binding.
[a] $n = 2$.

Table 9
Mutagenic activity of the test compounds, assessed by use of the *V. harveyi* test

Compound	BB7	BB7X	BB7M	BB7XM
	Number of colonies (mean ± SD)[b]			
CTR1[a]	13 ± 3	15 ± 3	14 ± 2	14 ± 4
CTR2[a]	14 ± 3	16 ± 1	13 ± 5	14 ± 5
NQNO	37 ± 2	31 ± 1	45 ± 4	33 ± 1
13	22 ± 2	17 ± 1	26 ± 4	23 ± 3
20	22 ± 4	27 ± 4	25 ± 7	20 ± 4
21	24 ± 5	29 ± 7	27 ± 9	19 ± 6
22a	20 ± 3	25 ± 4	22 ± 5	18 ± 8
23	15 ± 2	22 ± 2	26 ± 5	18 ± 3
25	20 ± 5	26 ± 5	20 ± 6	27 ± 4
26	28 ± 8	27 ± 5	26 ± 7	22 ± 5
27	29 ± 2	25 ± 5	26 ± 2	22 ± 4
28	22 ± 2	16 ± 4	18 ± 4	26 ± 5
29	25 ± 5	24 ± 5	19 ± 7	24 ± 3
30	20 ± 8	15 ± 5	10 ± 5	26 ± 7

[a] CTR1 (H_2O)—negative control; CTR2 (DMSO)—negative control; NQNO (nitroquinoline-*N*-oxide, 40 ng/mL)—positive control.
[b] Mean values from three experiments ± standard deviation (SD) are presented.

Table 10
Antimutagenic activity of the test compounds, assessed by use of the *V. harveyi* test

Compound[a]	BB7		BB7X		BB7M		BB7XM	
	Number of colonies: mean ± SD (inhibition rate %)[b]							
CTR1	16 ± 3		11 ± 1		14 ± 4		14 ± 4	
CTR2	12 ± 4		13 ± 2		16 ± 2		14 ± 1	
NQNO	38 ± 2		31 ± 2		45 ± 11		31 ± 3	
21	11 ± 3	(70)	23 ± 5	(27)	11 ± 1	(75)	16 ± 4	(48)
22a	9 ± 2	(75)	29 ± 3	(7)	14 ± 3	(69)	18 ± 4	(41)
23	11 ± 3	(70)	29 ± 4	(6)	14 ± 2	(69)	29 ± 12	(5)
25	4 ± 2	(81)	14 ± 4	(56)	20 ± 22	(55)	22 ± 4	(30)
26	5 ± 2	(88)	24 ± 4	(22)	22 ± 2	(52)	27 ± 3	(15)
27	7 ± 1	(82)	15 ± 1	(52)	11 ± 2	(75)	21 ± 3	(33)
28	6 ± 2	(84)	27 ± 3	(12)	30 ± 5	(34)	23 ± 6	(26)
29	7 ± 2	(81)	19 ± 3	(38)	17 ± 4	(62)	18 ± 2	(43)
30	15 ± 3	(62)	59 ± 7	(0)	33 ± 5	(27)	34 ± 3	(0)

[a] CTR1 (H_2O)—negative control; CTR2 (DMSO)—negative control; NQNO (nitroquinoline-*N*-oxide, 40 ng/mL)—positive control.
[b] Mean values from three experiments ± standard deviation (SD) are presented. The values in parenthesis are the inhibition rates (%) of mutagenicity; 25–40% inhibition: moderate antigenotoxicity, 40% or more inhibition: strong antigenotoxicity, 25% or less inhibition: no antigenotoxicity.

use of crystallography and compared with the reference compounds.

The most active compound is *R*-(−)-2*N*-{2-[2-(2,6-dimethylphenoxy)ethoxy]ethyl}aminopropan-1-ol hydrochloride (**22a**) (the ethoxyethyl analog of the reference compound II), exhibiting interesting anticonvulsant activity in MES and 6 Hz test (mice, *ip*), pilocarpine-induced status epilepticus (rats, *ip*) as well

Table 11
Summary of mutagenicity and antimutagenicity of tested compounds

Compound	Mutagenicity[a]				Antimutagenicity[b]			
	BB7	BB7X	BB7M	BB7XM	BB7	BB7X	BB7M	BB7XM
21	–	–	–	–	S	M	S	S
22a	–	–	–	–	S	0	S	S
23	–	–	–	–	S	0	S	0
25	–	–	–	–	S	S	S	M
26	–	–	–	–	S	W	S	W
27	–	–	–	–	S	S	S	M
28	–	–	–	–	S	W	M	M
29	–	–	–	–	S	M	S	S
30	–	–	–	–	S	0	M	0

[a] Positive result of the mutagenicity assay (+) indicates at least twofold increase in the number of neomycin-resistant colonies relative to the control experiment and/or the number of colonies higher than that observed in the experiment with a known mutagen (NQNO). Otherwise, the result is considered negative (−).
[b] Abbreviations are as follows: S—strong antimutagenic properties (>40% inhibition of mutagenicity of NQNO); M—moderate antimutagenic properties (25–40% inhibition of mutagenicity of NQNO); W—weak antimutagenic properties (10–25% inhibition of mutagenicity of NQNO); 0—no antimutagenic properties (<10% inhibition of mutagenicity of NQNO).

Table 12
Metabolic stability screen of compounds **22a**, **23** and **29** in mouse liver microsomes (MLMs) and major metabolites characteristics

Compound	$t_{1/2}$ [min]	Molecular ions (m/z)	Retention time (min)	Cl_{int} (μL/mg/min)	Metabolites			
					ID	Retention time (min)	% content among metabolites	Molecular ions (m/z)
22a	37	268	3.81	47	M1	2.81	72	284 $[M+16]^+$
					M2	2.73	28	300 $[M+32]^+$
23	37	268	3.80	47	M1	2.81	70	284 $[M+16]^+$
					M2	2.50	17	284 $[M+16]^+$
					M3	2.72	13	300 $[M+32]^+$
29	136	282	4.31	13	M1	2.57	61	298 $[M+16]^+$
					M2	3.34	20	298 $[M+16]^+$
					M3	4.17	19	224 $[M-58]^+$
Imipramine[16]	11	–	–	126				
Fentanyl[16]	39	–	–	89				

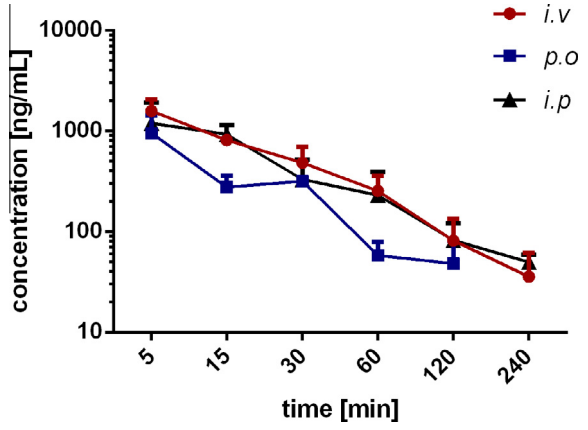

Figure 6. Plasma concentration–time profiles of compound **22a** following its intravenous, intragastric or intraperitoneal administration in mice (semi-logarithmic plots).

Table 13
Basic pharmacokinetic parameters of compound **22a** after its single intravenous, intragastric, or intraperitoneal administration in mice

Parameters	Administration		
	iv	*p.o.*	*ip*
C_0 (ng/mL)	2205	–	–
C_{max} (ng/mL)	–	950	1190
t_{max} (min)	–	5	5
$t_{1/2}$ (min)	51.5	29.1	77.2
MRT (min)	55.6	40.3	85.2
$AUC_{0\to\infty}$ (ng min/mL)	61,832.7	23,769.6	54,175.6
$AUMC_{0\to\infty}$ (ng min^2/mL)	3,439,871	958,477	4,614,684
Cl_t (mL/min/kg)	16.2	–	–
V_{ss} (mL/kg)	899.7	–	–
F (%)	–	2.98	6.78

C_0: the initial concentration, C_{max}: the maximum plasma concentration; t_{max}: time to reach the maximum plasma concentration; $t_{1/2}$: the terminal half-life; MRT: the mean residence time; $AUC_{0\to\infty}$: the area under the concentration–time curve from zero up to infinitive time; $AUMC_{0\to\infty}$: the area under the first-moment curve from zero up to infinitive time; Cl_t: the total clearance; V_{ss}: the volume of distribution at steady state; F: the absolute bioavailability.

as analgesic activity in a neurogenic pain model—the formalin test. The probable mechanism of action results from binding to some of σ, 5-HT_{2B}, 5-HT_{2A} receptors, or 5-HT transporter. The compound exhibits safety in *Vibrio harveyi* test tor mutagenesis. In terms of aim of the study—incorporation of ethoxyethyl linker instead of ethyl between phenoxyl and aminoalkanol resulted in interesting pharmacological profile.

During the study further questions arose, regarding metabolism and pharmacokinetics of the selected molecules. The results of undertaken efforts (metabolic stability and pharmacokinetic profile) prove that compound **22a** is metabolized mostly by the liver (rather than intestines), since the bioavailability after *ip* administration is not much higher (6.78%) compared to bioavailability after intragastric administration (2.98%). Taking into account the high activity of the compound in mice, we suppose that the formation of the active metabolites play an important role in the mechanism of action, compensating low bioavailability of the parent molecule.

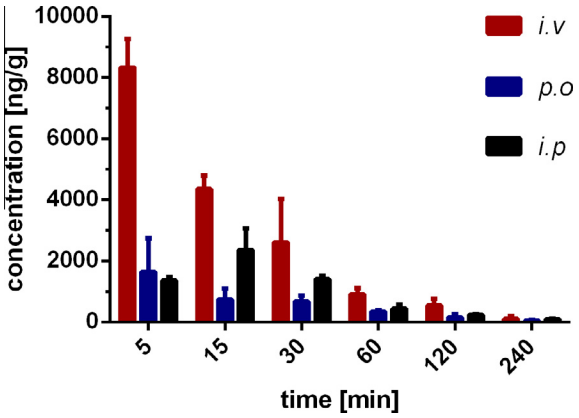

Figure 7. Distribution of **22a** to mice brain after its intravenous (1 mg/kg), intragastric (12.92 mg/kg), or intraperitoneal (12.92 mg/kg) administration.

Table 14
Distribution of **22a** in mice brain after intravenous, intragastric, or intraperitoneal administration

Parameters	*iv*	*po*	*ip*
$AUC_{0\rightarrow\infty}$ (ng min/g)	309,009	73,322	129,540
MRT (min)	50.1	73.8	83.1
C_{max} (ng/g)	11,527	1640	2360
t_{max} (min)	5	5	15

Table 15
Ratio of **22a** mean concentrations in brain and plasma after single intravenous, intragastric, or intraperitoneal administration

Time (min)	Ratio of **22a** concentrations in brain *versus* plasma		
	iv	*po*	*ip*
5	5.27	1.73	1.13
15	5.36	2.67	2.55
30	5.41	2.12	4.25
60	3.58	5.95	1.91
120	6.66	3.18	2.86
240	2.98		1.94

4. Experimental protocols

4.1. Chemistry

The aminoalkanols used for synthesis of compounds **1**, **3**–**4**, **6**–**8**, **11**–**12**, **14**, **16**, **18**–**19**, **21**, **24**, **27**, **30** were racemic (Table 1). D,L-*trans*-2-Aminocyclohexan-1-ol was achieved from cyclohexene oxide according to formerly published procedures.[7,17] All other reagents were purchased from Alfa Aesar GmbH & Co KG (Karlsruhe, Germany) and Merck Sp. z o.o. (Warszawa, Poland) and solvents were commercially available materials of reagent grade.

4.1.1. Synthesis of the title compounds

0.025 mole of appropriate bromide (*i.e.* (2,3-dimethylphenoxy) ethyl bromide, (2,3-dimethylphenoxy)propyl bromide, (2,4-dimethylphenoxy)ethyl bromide, (2,4,6-trimethylphenoxy)ethyl bromide, (2,3-dimethylphenoxy)ethoxyethyl bromide, (2,6-dimethylphenoxy)ethoxyethyl bromide, or (2,4,6-trimethylphenoxy)ethoxyethyl bromide) was placed in a 250 mL flask and 0.022 mole of appropriate aminoalkanol was added with 0.02 mol anhyd K_2CO_3 as proton acceptor. The mixture was refluxed in 50 mL toluene for 5 h, and afterwards the reaction mixture was filtered off (KBr/K_2CO_3) and the filtrate was subject to distillation under reduced pressure, until oily residue. Then 50 mL of water and l0% HCl was added until acidic pH, and the mixture was refluxed with activated carbon. Then the suspension was filtered off and 10% NaOH was added for alkalization of the filtrate and precipitation of the base. The oily product was extracted to toluene and the organic phase was dried with anhyd Na_2SO_4 overnight and the solvent was distilled off. The oily residue was recrystallized with use of *n*-hexane or petroleum ether for achievement of required crystal forms. The yield of N-alkylation ranged 45–75%. The yield of the method of N-alkylation with use of TEBA in acetone for several compounds ranged 35–60%.

In cases of **22a** or **23a** the bases were transformed into hydrochlorides with use of acetone solution of gaseous HCl. The obtained hydrochlorides were recrystallized from mixture acetone/MeOH (3:1).

Melting points (mp) were determined using a Büchi SMP-20 apparatus and are uncorrected. Analyses of C, H, N were within ±0.4% of the theoretical values. Analytical TLC was carried out on precoated plates (silica gel, 60 F-254 Merck). Spots were visualized with UV light. ^{1}H NMR and ^{13}C NMR spectra for compounds ^{1}H NMR and ^{13}C NMR spectra for compounds **1**–**3**, **6**–**8**, and **11**, **20**–**21** were recorded at Faculty of Chemistry, Jagiellonian University (Krakow, Poland), on a Bruker AVANCE III 600 (resonance frequencies 600.20 MHz for ^{1}H and 150.94 MHz for ^{13}C) equipped a 5-mm probehead: PABBO with z-gradient or TBI with XYZ gradients. The ^{1}H spectra were recorded with 16 scans, 1 s relaxation delay, 4 s acquisition time, 128 kW FID size, with 16,234 Hz spectral width. The ^{13}C spectra were recorded with WALTZ-16 ^{1}H broadband decoupling, a few thousands scans, 2 s relaxation delay, 0.9 s acquisition time, 64 kW FID size, 36,057 Hz spectral width. Standard pulse sequences from Bruker library were used for 2D spectra. Gradient enhanced sequences were used for the homo- and heteronuclear 2D experiments. All processing and analysis were performed using Bruker's TopSpin 3.0 software suite.

^{1}H NMR spectra for compounds ^{1}H NMR spectra for compounds **4**–**5**, **9**–**10**, **12**–**19**, **22**–**30** were recorded in $CDCl_3$ and **15a** and **23a**—in DMSO-d_6 were recorded at Faculty of Pharmacy, Jagiellonian University Medical College (Krakow, Poland) with a Varian Mercury-VX 300 NMR spectrometer at 29 °C. Chemical shifts were referenced against solvent lock signal. Standard Varian pulse sequences were used for 2D experiments.

Results are presented in the following format: chemical shift δ (ppm), multiplicity, *J* values in Hertz (Hz), number of protons, protons' position. Multiplicities are showed as the abbreviations: s (singlet), br s (broad singlet), d (doublet), dd (doublet of doublets), dt (doublet of triplets), t (triplet), tt (triplet of triplets), m (multiplet).

The IR spectra were recorded on a Jasco FT/IR 410 spectrometer (KBr pellets). Measurement of optical rotation ($[\alpha]_{589}$) was carried out using Jasco 2000 (λ = 589 nm). For mass spectrometry analysis samples were prepared in acetonitrile/water (10/90 v/v) mixture. The LC/MS system consisted of a Waters Acquity UPLC, coupled to a Waters TQD mass spectrometer (electrospray ionization mode ESI-tandem quadrupole). All the analyses were carried out usingan Acquity UPLC BEH C18, 1.7 lm, 2.1 × 100 mm column. A flow rate of 0.3 mL/min and a gradient of (5–95)% B over 10 min and then 100% B over 2 min was used. Eluent A: water/0.1% HCO_2H; eluent B: acetonitrile/0.1% HCO_2H. LC/MS data were obtained by scanning the first quadrupole in 0.5 s in a mass range from 50 to 1000 Da; eight scans were summed up to produce the final spectrum.

4.1.1.1. *R,S*-2*N*-[(2,3-Dimethylphenoxy)ethyl]aminopropan-1-ol (1). White solid. Yield = 60%. *M* = 223.31; $C_{13}H_{21}NO_2$; mp 76–78 °C [$\%^{calcd}/_{analyzed}$] $C^{69.92}/_{69.45}$, $H^{9.48}/_{9.73}$ $N^{6.27}/_{6.24}$; R_f = 0.47 (CH_3OH); IR (KBr, cm^{-1}) *v*: 3735, 3649, 3295, 3127, 2964, 2931, 2886, 2833, 2601, 2361, 2116, 1909, 1587, 1461, 1266, 771; ^{1}H NMR (δ

ppm): 7.01 (dd, *J* = 7.9, *J* = 7.5, 1H, H-5); 6.77 (d, *J* = 7.9, 1H, H-4); 6.74 (d, *J* = 7.5, 1H, H-6); 4.54 (t, *J* = 5.2, 1H, OH); 4.03–3.97 (m, 1H, C*H*H–OAr); 3.97–3.91 (m, 1H, CH*H*–OAr); 3.27–3.24 (m, 1H, C*H*H–OH); 3.24–3.17 (m, 1H, CH*H*–OH); 2.97–2.90 (m, 1H, C*H*H–N); 2.90–2.83 (m, 1H, CH*H*–N); 2.71–2.62 (m, 1H, CH); 2.20 (s, 3H, CH_3–Ar (2)); 2.07 (s, 3H, CH_3–Ar (3)); 1.89 (br s, 1H, NH); 0.92 (d, *J* = 6.4, 3H, CH_3).

4.1.1.2. 2*N*-[(2,3-Dimethylphenoxy)ethyl]amino-2-methylpropan-1-ol (2). White solid. Yield = 62%; *M* = 237.34; $C_{14}H_{23}NO_2$; mp 75–77 °C; [%^{calcd}/$_{analyzed}$] $C^{70.85}/_{70.70}$, $H^{9.77}/_{9.90}$, $N^{5.90}/_{5.72}$; R_f = 0.44 (CH_3OH); IR (KBr, cm^{-1}) *ν*: 3295, 3154, 2986, 2971, 2926, 2877, 2827, 2756, 2557, 2359, 1584, 1464, 1263, 1068, 768; ^{1}H NMR (*δ* ppm): 7.05 (dd, *J* = 8.0, *J* = 7.5, 1H, H-5); 6.80 (d, *J* = 8.0, 1H, H-6); 6.78 (d, *J* = 7.5, 1H, H-4); 4.68 (t, *J* = 3.1, 1H, OH); 3.98 (t, *J* = 5.7, 2H, CH_2–OAr); 3.24 (d, *J* = 3.1, 2H, C*H*$_2$–OH); 2.86 (t, *J* = 5.7, 2H, CH_2–N); 2.24 (s, 3H, CH_3–Ar (3)); 2.12 (s, 3H, CH_3–Ar (2)); 1.82 (br s, 1H, NH); 1.01 (s, 6H, 2× CH_3).

4.1.1.3. *R,S*-2*N*-[(2,3-Dimethylphenoxy)ethyl]aminobutan-1-ol (3). White solid. Yield = 55%; *M* = 237.34; $C_{14}H_{23}NO_2$; mp 55–56 °C; [%^{calcd}/$_{analyzed}$] $C^{70.86}/_{70.76}$, $H^{9.77}/_{9.76}$, $N^{5.90}/_{5.82}$; R_f = 0.51 (CH_3-OH); IR (KBr, cm^{-1}) *ν*: 3295, 3158, 2964, 2931, 2875, 2837, 1900, 1585, 1470, 1263, 1109, 1062, 762; ^{1}H NMR (*δ* ppm): 7.01 (dd, *J* = 8.3, *J* = 7.7, 1H, H-5); 6.77 (d, *J* = 8.3, 1H, H-6); 6.74 (d, *J* = 7.7, 1H, H-4); 4.46 (t, *J* = 4.4, 1H, OH); 3.98 (dt, *J* = 9.5, *J* = 5.5, 1H, C*H*H–OAr); 3.94 (dt, *J* = 9.5, *J* = 5.5, 1H, CH*H*–OAr); 3.43–3.20 (m, 2H, C*H*$_2$–OH); 2.90 (t, *J* = 5.5, 2H, CH_2–N); 2.49–2.41 (m, 1H, CH); 2.20 (s, 3H, CH_3–Ar (2)); 2.07 (s, 3H, CH_3–Ar (3)); 1.81 (br s, 1H, NH); 1.41–1.31 (m, 2H, CH_2–CH_3); 0.85 (t, *J* = 7.3, 3H, CH_2–C*H*$_3$).

4.1.1.4. D,L-*trans*-2*N*-[(2,3-Dimethylphenoxy)ethyl]aminocyclohexan-1-ol (4). White solid. Yield = 57%; *M* = 263.38; $C_{16}H_{25}NO_2$; mp 95–97 °C; [%^{calcd}/$_{analyzed}$] $C^{72.97}/_{72.71}$, $H^{9.57}/_{9.26}$, $N^{5.32}/_{5.23}$; R_f = 0.54 (CH_3OH/ethyl acetate 1:1); IR (KBr, cm^{-1}) *ν*: 3298, 3113, 2929, 2858, 2816, 2365, 1585, 1461, 1264, 1111; ^{1}H NMR (*δ* ppm): 6.97–7.09 (m, 1H, Ar–H5); 6.78 (d, *J* = 7.69, 1H, Ar–H4); 6.71 (d, *J* = 8.21, 1H, Ar–H6); 4.05 (t, *J* = 5.26, 2H, O–C*H*$_2$–CH_2–NH); 3.33 (br s, 1H, NH); 3.27–3.10 (m, 2H, O–CH_2–C*H*$_2$–NH); 2.89 (dt, *J* = 12.50, *J* = 4.78, 1H, C*H*–OH); 2.27 (s, 3H, CH_3–Ar (2)); 2.34–2.22 (m, 1H, C*H*–NH); 2.15 (s, 3H, CH_3–Ar (3)); 2.13–2.00 (m, 2H, cyclohex); 1.80–1.67 (m, 2H, cyclohex); 1.35–1.17 (m, 3H, cyclohex); 1.09–0.92 (m, 1H, cyclohex).

4.1.1.5. *N*-[(2,3-Dimethylphenoxy)ethyl]piperidin-4-ol (5). White solid. Yield = 53%; *M* = 249.35; $C_{15}H_{23}NO_2$; mp 71–72 °C; [%^{calcd}/$_{analyzed}$] $C^{72.25}/_{72.44}$, $H^{9.30}/_{9.10}$, $N^{5.62}/_{5.59}$; R_f = 0.47 (CH_3OH/ethyl acetate 1:1); IR (KBr, cm^{-1}) *ν*: 3153, 2974, 2943, 2912, 2866, 2798, 2688, 2599, 2503, 1581, 1459, 1254, 998; ^{1}H NMR (*δ* ppm): 7.04 (t, *J* = 7.9, 1H, Ar–H5); 6.78 (d, *J* = 7.8, 1H, Ar–H4); 6.70 (d, *J* = 8.2, 1H, Ar–H6); 4.08 (t, *J* = 5.9, 2H, Ar–O–C*H*$_2$); 3.74–3.68 (m, 1H, C*H*–OH); 2.93–2.88 (m, 2H, pip); 2.84 (t, *J* = 5.6, 2H, C*H*$_2$–N); 2.37–2.29 (m, 2H, pip); 2.27 (s, 3H, CH_3–Ar); 2.14 (s, 3H, CH_3–Ar); 1.95–1.87 (m, 2H, pip); 1.68–1.54 (m, 2H, pip).

4.1.1.6. *R,S*-2*N*-[(2,3-Dimethylphenoxy)ethyl]amino-1-phenylethan-1-ol (6). White solid. Yield = 67%; *M* = 285.38; $C_{18}H_{23}NO_2$; mp 118–120 °C; [%^{calcd}/$_{analyzed}$] $C^{75.75}/_{75.83}$, $H^{8.12}/_{8.28}$, $N^{4.91}/_{4.82}$; R_f = 0.62 (CH_3OH); *c*Log*P* = 3.03; IR (KBr, cm^{-1}) *ν*: 3310, 3064, 3033, 2975, 2921, 2899, 2871, 2836, 2735, 2519, 2364, 1892, 1588, 1453, 1266, 1108, 762; ^{1}H NMR (*δ* ppm): 7.39–7.18 (m, 5H, H-2′-H6′); 7.01 (dd, *J* = 8.2, *J* = 7.6, 1H, H-5); 6.76 (d, *J* = 8.2, 1H, H-6); 6.73 (d, *J* = 7.6, 1H, H-4); 5.30 (br s, 1H, –OH); 4.65 (t, *J* = 6.3, 1H, CH); 3.97 (t, *J* = 5.5, 2H, Ar–O–CH_2–); 2.92 (t, *J* = 5.5, 2H, –CH_2–N); 2.73 (d, *J* = 6.3, 2H, N–CH_2–); 2.20 (s, 3H, CH_3–Ar (3)); 2.03 (s, 3H, CH_3–Ar (2)); 1.92 (br s, 1H, –NH); ^{13}C NMR (*δ* ppm): 156.37 (C-1), 144.54 (C-1′), 137.15 (C-3), 127.90 (C-3′, C-5′), 126.75 (C-4′), 125.89 (C-2′, C-6′), 125.85 (C-5), 124.19 (C-2), 122.01 (C-4), 109.29 (C-6), 71.61 (CH), 67.93 (Ar–O–CH_2–), 57.54 (N–CH_2–), 48.17 (–CH_2–N), 19.69 (CH_3–Ar (3)), 11.37 (CH_3–Ar (2)).

4.1.1.7. *R,S*-2*N*-[(2,3-Dimethylphenoxy)propyl]aminopropan-1-ol (7). White solid. Yield = 64%; *M* = 237.34; $C_{14}H_{23}NO_2$; mp 88–90 °C; [%^{calcd}/$_{analyzed}$] $C^{70.85}/_{70.89}$, $H^{9.77}/_{10.02}$, $N^{5.90}/_{5.86}$; R_f = 0.24 (CH_3OH); IR (KBr, cm^{-1}) *ν*: 3260, 3110, 2957, 2924, 2824, 2599, 2359, 1593, 1481, 1257, 1091, 768; ^{1}H NMR (*δ* ppm): 7.00 (dd, *J* = 8.2, *J* = 7.5, 1H, H-5); 6.76 (d, *J* = 8.5, 1H, H-4); 6.73 (d, *J* = 7.5, 1H, H-6); 4.45 (br s, 1H, OH); 3.91 (t, *J* = 6.2, 2H, CH_2–OAr); 3.28–3.18 (m, 2H, C*H*$_2$–OH); 2.80–2.70 (m, 2H, CH_2–N); 2.69–2.55 (m, 1H, CH); 2.20 (s, 3H, CH_3–Ar (2)); 2.07 (s, 3H, CH_3–Ar (3)); 1.87–1.80 (m, 2H, R–CH_2–R); 1.56 (br s, 1H, NH); 0.90 (d, *J* = 6.4, 3H, CH_3).

4.1.1.8. *R,S*-2*N*-[(2,3-Dimethylphenoxy)propyl]aminobutan-1-ol (8). White solid. Yield = 60%; *M* = 251.37; $C_{15}H_{25}NO_2$; mp 82–84 °C; [%^{calcd}/$_{analyzed}$] $C^{71.67}/_{71.43}$, $H^{10.02}/_{10.01}$, $N^{5.57}/_{5.53}$; R_f = 0.24 (CH_3OH); IR (KBr, cm^{-1}) *ν*: 3258, 3100, 2964, 2922, 2863, 2815, 1910, 1584, 1464, 1255, 1096, 768; ^{1}H NMR (*δ* ppm): 7.00 (dd, *J* = 8.2; *J* = 7.6, 1H, H-5); 6.77 (d, *J* = 8.2, 1H, H-6); 6.70 (d, *J* = 7.6, 1H, H-4); 4.40 (br s, 1H, –OH); 3.99 (t, *J* = 6.2, 2H, Ar–O–CH_2–); 3.39–3.21 (m, 2H, C*H*$_2$–OH); 2.69 (t, *J* = 6.8, 2H, –CH_2–N); 2.41–2.31 (m, 1H, CH); 2.20 (s, 3H, CH_3–Ar (3)); 2.07 (s, 3H, CH_3–Ar (2)); 1.84 (tt, *J* = 6.8, *J* = 6.2, 2H, R–CH_2–R); 1.48 (br s, 1H, –NH); 1.39–1.28 (m, 2H, –C*H*$_2$–CH_3); 0.83 (t, *J* = 7.5, 3H, R–CH_3); ^{13}C NMR (*δ* ppm): 156.40 (C-1), 137.02 (C-3), 125.77 (C-5), 124.03 (C-2), 121.75 (C-4), 109.07 (C-6), 65.96 (Ar–O–CH_2–), 62.47 (C*H*$_2$–OH), 60.22 (CH), 43.42 (–CH_2–N), 29.93 (R–CH_2–R), 23.60 (CH_3–C*H*$_2$–), 19.64 (CH_3–Ar(3)), 11.29 (CH_3–Ar(2)), 9.94 (CH_3–CH_2–).

4.1.1.9. *N*-[(2,3-Dimethylphenoxy)propyl]piperidin-3-ol (9). White solid. Yield = 53%; *M* = 263.38; $C_{16}H_{25}NO_2$; mp 86–88 °C; [%^{calcd}/$_{analyzed}$] $C^{72.97}/_{72.48}$, $H^{9.57}/_{9.45}$, $N^{5.32}/_{5.25}$; R_f = 0.54 (CH_3OH/ethyl acetate 1:1); *c*Log*P* = 2.76; IR (KBr, cm^{-1}) *ν*: 3149, 2947, 2867, 2826, 2775, 2513, 2149, 1914, 1584, 1467, 1068; ^{1}H NMR (*δ* ppm): 7.08–6.99 (m, 1H, Ar–H5); 6.77 (d, *J* = 7.44, 1H, Ar–H4); 6.70 (d, *J* = 8.21, 1H, Ar–H6); 3.99 (t, *J* = 6.28, 2H, O–C*H*$_2$–CH_2–CH_2–NH); 3.82 (br s, 1H, NH); 2.61–2.45 (m, 5H, O–CH_2–CH_2–C*H*$_2$–NH, C*H*–OH, pip-H); 2.42 (br s, 1H, OH); 2.36–2.28 (m, 1H, pip-H); 2.27 (s, 3H, CH_3–Ar (2)); 2.14 (s, 3H, CH_3–Ar (3)); 2.04–1.90 (m, 2H, O–CH_2–C*H*$_2$–CH_2–NH); 1.88–1.72 (m, 1H, pip); 1.69–1.46 (m, 3H, pip).

4.1.1.10. 1*N*-[(2,3-Dimethylphenoxy)propyl]piperidin-4-ol (10). White solid. Yield = 56%; *M* = 263.38; $C_{16}H_{25}NO_2$; mp 68–70 °C; [%^{calcd}/$_{analyzed}$] $C^{72.97}/_{73.15}$, $H^{9.57}/_{9.42}$, $N^{5.32}/_{5.29}$; R_f = 0.39 (CH_3-OH/ethyl acetate 1:1); *c*Log*P* = 2.74; IR (KBr, cm^{-1}) *ν*: 3133, 2959, 2874, 2818, 2802, 2748, 2362, 2140, 1900, 1582, 1468, 1261; ^{1}H NMR (*δ* ppm): 7.08–6.99 (m, 1H, Ar–H5); 6.76 (d, *J* = 7.44, 1H, Ar–H4); 6.70 (d, *J* = 8.21, 1H, Ar–H6); 3.99 (t, *J* = 6.16, 2H, O–C*H*$_2$–CH_2–CH_2–NH); 3.71 (m, 1H, C*H*–OH); 2.91–2.73 (m, 2H, pip); 2.61–2.47 (m, 2H, O–CH_2–CH_2–C*H*$_2$–NH); 2.26 (s, 3H, CH_3–Ar (2)); 2.22–2.15 (m, 2H, pip); 2.14 (s, 3H, CH_3–Ar (3)); 2.07–1.84 (m, 4H, pip); 1.66–1.52 (m, 2H, O–CH_2–C*H*$_2$–CH_2–NH); 1.47 (br s, 1H, OH).

4.1.1.11. *R,S*-2*N*-[(2,3-Dimethylphenoxy)propyl]amino-1-phenylethan-1-ol (11). White solid. Yield = 62%; *M* = 299.42; $C_{19}H_{25}NO_2$; mp 111–112 °C; [%^{calcd}/$_{analyzed}$] $C^{76.22}/_{76.21}$, $H^{8.42}/_{8.43}$, $N^{4.68}/_{4.63}$; R_f = 0.38 (CH_3OH); IR (KBr, cm^{-1}) *ν*: 3333, 3322, 3063, 3030, 2946, 2922, 2895, 2844, 2754, 1953, 1582, 1256, 1102, 703; ^{1}H NMR (*δ* ppm): 7.38–7.16 (m, 5H, H-2′ H-6′); 7.01 (dd, *J* = 8.1, *J* = 7.6, 1H, H-5); 6.75 (d, *J* = 8.1, 1H, H-6); 6.73 (d, *J* = 7.6, 1H, H-4), 5.24 (br s, 1H, –OH); 4.62 (t, *J* = 6.5, 1H, CH); 3.97 (t, *J* = 6.3, 2H, Ar–O–CH_2–); 2.72 (t, *J* = 6.9, 2H, –CH_2–N); 2.64 (d,

J = 6.5, 2H, N–CH_2–); 2.20 (s, 3H, CH_3–Ar (3)); 2.06 (s, 3H, CH_3–Ar (2)); 1.85 (tt, J = 6.9, J = 6.3, 2H, R–CH_2–R); 1.72 (br s, 1H, –NH); ^{13}C NMR (δ ppm): 156.36 (C-1), 144.58 (C-1′), 137.01 (C-3), 127.78 (C-3′, C-5′), 126.62 (C-4′), 125.78 (C-2′, C-6′), 125.75 (C-5), 124.02 (C-2), 121.75 (C-4), 109.04 (C-6), 71.41 (CH), 65.91 (Ar–O–CH_2–), 57.73 (N–CH_2–), 45.86 (–CH_2–N), 29.43 (R–CH_2–R), 19.63 (CH_3–Ar (3)), 11.31 (CH_3–Ar (2)).

4.1.1.12. *R,S*-2*N*-[(2,4-Dimethylphenoxy)ethyl]aminopropan-1-ol (12). White solid. Yield = 70%; M = 223.31; $C_{13}H_{21}NO_2$; mp 60–61 °C; [%^{calcd}/$_{analyzed}$] $C^{69.92}/_{70.14}$, $H^{9.48}/_{9.42}$, $N^{6.27}/_{6.22}$; R_f = 0.44 (CH_3-OH/$CHCl_3$ 1:9), R_f = 0.49 (CH_3OH/ethyl acetate 1:1); IR (KBr, cm^{-1}) ν: 3296, 3119, 3018, 2961, 2917, 2838, 2729, 2603, 1505, 1461, 1252, 1223, 1050, 791; ^{1}H NMR (δ ppm): 6.95–6.92 (m, 2H, H–Ar (3,5)); 6.72 (d, J = 7.9, 1H, H–Ar (6)); 4.07–4.00 (m, 2H, Ar–O–CH_2); 3.60 (dd, J = 4.1, J = 10.5, 1H, C*H*H–OH); 3.27 (dd, J = 6.9, J = 10.5, 1H, CH*H*–OH); 3.17–3.09 (m, 1H, C*H*H–N); 2.96–2.82 (m, 2H, CH + CH*H*–N); 2.26 (s, 3H, CH_3–Ar); 2.19 (s, 3H, CH_3–Ar); 1.09 (d, J = 6.4, 3H, CH–CH_3).

4.1.1.13. *R*-(−)-2*N*-[(2,4-Dimethylphenoxy)ethyl]aminopropan-1-ol (13). White solid. Yield = 70%; M = 223.31; $C_{13}H_{21}NO_2$; mp 69–71 °C; R_f = 0.40 (CH_3OH/$CHCl_3$ 1:9), R_f = 0.50 (CH_3OH/ethyl acetate 1:1); IR (KBr, cm^{-1}) ν: 3299, 3170, 2969, 2923, 2842, 2733, 1613, 1506, 1255, 1048; ^{1}H NMR (δ ppm): 6.95–6.92 (m, 2H, H–Ar (3,5)); 6.72 (d, J = 7.9, 1H, H–Ar(6)); 4.07–4.00 (m, 2H, Ar–O–CH_2); 3.61 (dd, J = 4.1, J = 10.5, 1H, C*H*H–OH); 3.17–3.09 (m, 1H, C*H*HN); 2.96–2.82 (m, 2H, C*H*–CH_3, CH*H*–N); 2.27 (dd, J = 6.9, J = 10.5, 1H, CH*H*–OH); 2.25 (s, 3H, CH_3–Ar); 2.19 (s, 3H, CH_3–Ar); 1.09 (d, J = 6.4, 3H, CH–CH_3); LC–MS $[M+H]^+$ m/z:8 224.33, 99.34%; $[\alpha]_D^{20}$ = −15.75° (CH_3OH, c 2%).

4.1.1.14. *R,S*-2*N*-[(2,4,6-Trimethylphenoxy)ethyl]aminopropan-1-ol (14). White solid. Yield = 64%; M = 237.33; $C_{14}H_{23}NO_2$; mp 80–82 °C; [%^{calcd}/$_{analyzed}$] $C^{70.85}/_{69.95}$, $H^{9.77}/_{9.52}$, $N^{5.90}/_{5.98}$; R_f = 0.41 (EtOH/ethyl acetate 1:1); ^{1}H NMR (δ ppm): 6.80 (s, 2H, Ar–H), 4.56 (br s, 1H, OH), 3.78–3.69 (m, J = 5.5, J = 5.5, J = 2.6, 2H, Ar–O–CH_2), 3.43–3.16 (m, 3H, CH_2–OH + NH–C*H*), 2.94–2.78 (m, 2H, CH_2–N), 2.73–2.60 (m, 1H, NH), 2.17 (s, 9H, CH_3–Ar), 0.93 (d, J = 6.4 Hz, 3H, CH–CH_3).

4.1.1.15. *R*-(−)-2*N*-[(2,4,6-Trimethylphenoxy)ethyl]aminopropan-1-ol (15). White solid. Yield = 60%; M = 237.33; $C_{14}H_{23}NO_2$; mp 91–92 °C; [%^{calcd}/$_{analyzed}$] $C^{70.85}/_{71.15}$, $H^{9.77}/_{9.86}$, $N^{5.90}/_{5.92}$; R_f = 0.40 (EtOH/ethyl acetate 1:1); ^{1}H NMR (dmso,300 MHz): δ (ppm) 6.78 (s, 2H, Ar–H), 4.54 (t, J = 5.3 Hz, 1H, OH), 3.64–3.79 (m, 2H, –O–CH_2–), 3.26–3.33 (m, 2H, –CH_2–OH), 3.16–3.25 (m, 1H, CH), 2.80–2.88 (m, 1H, –CH*H*–NH–), 2.65 (q, J = 5.1x(3) Hz, 1H, NH), 2.48 (dt, J = 3.7, 1.7 Hz, 1H, –CH*H*–NH–), 2.15 (s, 9H, Ar–CH_3), 0.91 (d, J = 6.4 Hz, 3H, CH–CH_3); $[\alpha]_D^{20}$ = −34.4° (c 1%, $CHCl_3$); LC–MS $[M+H]^+$ m/z: 238.36, 100.0%.

4.1.1.16. D,L-*trans*-2*N*-[(2,4,6-Trimethylphenoxy)ethyl]aminocyclohexan-1-ol (16). White solid. Yield = 74%; M = 277.46; $C_{17}H_{27}NO_2$; mp 90–91 °C; [%^{calcd}/$_{analyzed}$] $C^{73.58}/_{72.80}$, $H^{9.81}/_{9.87}$, $N^{5.07}/_{4.95}$; R_f = 0.55 (CH_3OH/benzene 1:5); ^{1}H NMR (δ ppm): 6.80 (s, 2H, Ar–H); 4.63 (d, 1H, J = 5.1, OH); 3.80–3.69 (m, 2H, Ar–O–CH_2); 3.15–3.08 (m, 1H, C*H*–OH); 2.93–2.87 (m, 1H, CH*H*–N); 2.84–2.77 (m, 1H, CH*H*–N); 2.44 (br s, 1H, NH); 2.26–2.19 (m, 1H, N–CH); 2.17 (s, 6H, CH_3–Ar(2,6)); 2.17 (s, 3H, CH_3–Ar(4)); 1.96–1.87 (m, 1H, cyclohex); 1.85–1.76 (m, 1H, cyclohex); 1.85–1.54 (m, 2H, cyclohex); 1.27–1.10 (m, 3H, cyclohex); 0.98–0.88 (m, 1H, cyclohex).

4.1.1.17. *trans*-4*N*-[(2,4,6-Trimethylphenoxy)ethyl]aminocyclohexan-1-ol (17). White solid. Yield = 55%; M = 277.41; $C_{17}H_{27}NO_2$; mp 100–102 °C; [%^{calcd}/$_{analyzed}$] $C^{73.58}/_{73.54}$, $H^{9.81}/_{9.83}$, $N^{5.07}/_{4.98}$; IR (KBr, cm^{-1}) ν: 3411, 3298, 3142, 2927, 2857, 2833, 2360, 1606, 1465, 1213, 1148, 1069857, 626; ^{1}H NMR (δ ppm): 6.81 (s, 2H, H–Ar); 3.89 (t, J = 5.26, 2H, CH_2–O); 3.70–3.57 (m, 1H, >CH–OH); 3.03 (t, J = 5.26, 2H, CH_2–NH); 2.68–2.54 (m, 1H, >CH–NH); 2.24 (s, 9H, CH_3–Ar); 2.07–1.96 (m, 5H, cyclohex, OH, NH); 1.44–1.17 (m, 4H, cyclohex).

4.1.1.18. *R,S*-4*N*-[(2,4,6-Trimethylphenoxy)ethyl]amino-1-phenylethan-1-ol (18). White solid. Yield 58%; M = 299.47; $C_{19}H_{25}NO_2$; mp 120–121 °C; [%^{calcd}/$_{analyzed}$] $C^{76.20}/_{76.26}$, $H^{8.41}/_{8.65}$, $N^{4.70}/_{4.81}$; R_f = 0.58 (CH_3OH/benzene 1:5); ^{1}H NMR (δ ppm): 7.40–7.28 (m, 4H, H–Ar(2,3,5,6)); 7.26–7.20 (m, 1H, H–Ar(4)); 6.80 (s, 2H, H–Ar); 5.33 (d, 1H, J = 2.6, OH); 4.66 (d, 1H, J = 2.5, C*H*–OH); 3.73 (t, 2H, J = 5.3, Ar–O–CH_2); 2.84–2.82 (m, 2H, CH_2–N); 2.72 (d, 2H, J = 6.3, N–CH_2); 2.17 (s, 3H, CH_3–Ar(4)); 2.16 (s, 6H, CH_3–Ar(2,6)); 2.11 (br s, 1H, NH).

4.1.1.19. *R,S*-2*N*-{2-[2-(2,3-Dimethylphenoxy)ethoxy]ethyl}aminopropan-1-ol (19). White solid. Yield = 45%; M = 267.36; $C_{15}H_{25}NO_3$; mp 50–52 °C; [%^{calcd}/$_{analyzed}$] $C^{67.38}/_{67.42}$, $H^{9.42}/_{9.36}$, $N^{5.24}/_{5.11}$; R_f = 0.13 (CH_3OH/ethyl acetate 1:1); IR (KBr, cm^{-1}): 3255, 3095, 2962, 2918, 2853, 2692, 2585, 1584, 1479, 1260, 1107, 760; ^{1}H NMR (δ ppm): 7.04 (t, J = 7.7; 1H, Ar–H5); 6.78 (d, J = 7.4; 1H, Ar–H4); 6.72 (d, J = 8.2. 1H, Ar–H6); 4.11 (d, J = 4.6; 2H, Ar–O–CH_2); 3.87–3.82 (m, 2H, Ar–O–CH_2–CH_2); 3.72–3.65 (m, 2H, O–CH_2–CH_2–NH); 3.58 (dd, J = 10.5; J = 4.1; 1H, C*H*H–OH); 3.22 (dd, J = 10.5; J = 6.7; 1H, CH*H*–OH); 2.99–2.90 (m, 1H, O–CH_2–C*H*H–NH); 2.82–2.68 (m, 2H, O–CH_2–CH*H*–NH + NH–C*H*); 2.27 (s, 3H, CH_3–Ar); 2.16 (s, 3H, CH_3–Ar); 1.05 (d, J = 6.7; 3H, CH–CH_3); ^{13}C NMR (δ ppm): 156.31 (C-1′), 137.16 (C-3′), 125.78 (C-5′), 124.34 (C-2′), 122.09 (C-4′), 109.55 (C-6′), 70.63 (C-5), 68.88 (C-3), 67.67 (C-2), 65.49 (C-9), 54.37 (C-8), 46.26 (C-6), 19.62 (CH_3-3′), 17.16 (CH_3-8), 11.37 (CH_3-2′).

4.1.1.20. *trans*-4*N*-{2-[2-(2,3-Dimethylphenoxy)ethoxy]ethyl}aminocyclohexan-1-ol (20). White solid. Yield = 65%; M = 307.43; $C_{18}H_{29}NO_3$; mp 68–70 °C; [%^{calcd}/$_{analyzed}$] $C^{70.32}/_{70.69}$, $H^{9.50}/_{9.12}$, $N^{4.56}/_{4.33}$; ^{1}H NMR (δ ppm): 7.07 (dd, J = 8.1; J = 7.5; 1H, Ar–H5); 6.78 (d, J = 8.1; 1H, Ar–H6); 6.75 (d, J = 7.5; 1H, Ar–H4); 4.43 (br s, 1H, –OH); 4.04 (ddd, J = 6.2; J = 4.7; J = 3.2; 2H, Ar–O–CH_2); 3.71 (ddd, J = 6.2; J = 4.7; J = 3.2; 2H, Ar–O–CH_2–CH_2); 3.51 (t, J = 5.7; 2H, O–CH_2–CH_2–NH); 3.36–3.30 (m, 1H, C*H*–OH); 2.66 (t, J = 5.7; 2H, O–CH_2–CH_2–NH); 2.29 (tt, J = 10.6; J = 3.5; 1H, C*H*–NH); 2.20 (s, 3H, CH_3–Ar); 2.07 (s, 3H, CH_3–Ar); 1.80–1.73 (m, 4H, cyclohex); 1.40 (br s, 1H, –NH); 1.16–1.07 (m, 2H, cyclohex); 1.01–0.92 (m, 2H, cyclohex). ^{13}C NMR (δ ppm): 156.30 (C-1), 137.19 (C-3), 125.81 (C-5), 124.27 (C-2), 122.09 (C-4), 109.53 (C-6), 70.45 (–O–CH_2–CH_2–NH–), 68.83 (Ar–O–CH_2–CH_2–O–), 68.78 (CH–OH (cyclohex)), 67.62 (Ar–O–CH_2–CH_2–O–), 55.61 (CH–NH (cyclohex)), 46.10 (–O–CH_2–CH_2–NH–), 33.78 (C-3′, C-5′), 30.90 (C-2′, C-6′), 19.66 (CH_3–Ar (3)), 11.39 (CH_3–Ar (2)).

4.1.1.21. *R,S*-2*N*-{2-[2-(2,6-Dimethylphenoxy)ethoxy]ethyl}aminopropan-1-ol (21). White solid. Yield = 62%; M = 267.36; $C_{15}H_{25}NO_3$; mp 46–48 °C; [%^{calcd}/$_{analyzed}$] $C^{67.38}/_{67.21}$, $H^{9.42}/_{9.66}$, $N^{5.24}/_{5.12}$; IR (KBr, cm^{-1}): 3429, 3295, 2918, 2872, 1631, 1474, 1204, 1134, 1059, 756; ^{1}H NMR (δ ppm): 7.00 (d, J = 7.4; 2H, Ar–H3); 6.92 (dd, J = 8.1; J = 6.2, 1H, Ar–H4); 3.98–3.92 (m, 2H, Ar–O–CH_2); 3.84–3.78 (m, 2H, Ar–O–CH_2–CH_2); 3.74–3.67 (m, 2H, O–CH_2–CH_2–NH); 3.61 (dd, J = 10.5; J = 3.7; 1H, C*H*H–OH); 3.30 (dd, J = 11.2; J = 7.2; 1H, C*H*H–OH); 3.06–2.96 (m, 1H, O–CH_2–C*H*H–NH); 2.91–2.74 (m, 1H, O–CH_2–CH*H*–NH); 2.91–2.74 (m, 1H, NH–C*H*); 2.41 (br s, 2H, OH, NH); 2.29 (s, 6H, CH_3–Ar); 1.09 (d, J = 6.7; 3H, CH–CH_3), LC–MS $[M+H]^+$ m/z: 268.34, 97.92%.

4.1.1.22. *R*-(−)-2*N*-{2-[2-(2,6-Dimethylphenoxy)ethoxy]ethyl} aminopropan-1-ol (22). White solid. Yield = 60%; *M* = 267.36; $C_{15}H_{25}NO_3$; mp 46–48 °C; [%^{calcd}/$_{analyzed}$] C$^{67.38}$/$_{67.31}$, H$^{9.42}$/$_{9.70}$, N$^{5.24}$/$_{5.04}$; IR (KBr, cm^{-1}): 3423, 3301, 2915, 2869, 1475, 1203, 1137, 1061, 756; ^{1}H NMR (δ ppm): 7.00 (d, *J* = 7.4; 2H, Ar–H3); 6.92 (dd, *J* = 8.1; *J* = 6.2, 1H, Ar–H4); 3.98–3.92 (m, 2H, Ar–O–CH$_2$); 3.84–3.78 (m, 2H, Ar–O–CH$_2$–C*H*$_2$); 3.74–3.67 (m, 2H, O–C*H*$_2$–CH$_2$–NH); 3.61 (dd, *J* = 10.5; *J* = 3.7; 1H, C*H*H–OH); 3.30 (dd, *J* = 11.2; *J* = 7.2; 1H, CH*H*–OH); 3.06–2.96 (m, 1H, O–CH$_2$–CH*H*–NH); 2.91–2.74 (m, 1H, O–CH$_2$–C*H*H–NH); 2.91–2.74 (m, 1H, NH–C*H*); 2.41 (br s, 2H, OH, NH); 2.29 (s, 6H, CH$_3$–Ar); 1.09 (d, *J* = 6.7; 3H, CH–C*H*$_3$); $[\alpha]_D^{20}$ = −13.25° (CH$_3$OH, *c* 1%).

*4.1.1.22.1. R-(−)-2N-{2-[2-(2,6-Dimethylphenoxy)ethoxy]ethyl} aminopropan-1-ol hydrochloride (**22a**).* White solid. Yield = 85%; *M* = 303.82; $C_{15}H_{26}NO_3Cl$; mp 98–100 °C; [%^{calcd}/$_{analyzed}$] C$^{59.29}$/$_{58.98}$, H$^{8.63}$/$_{8.68}$, N$^{4.53}$/$_{4.59}$; IR (KBr, cm^{-1}): 3255, 3095, 2962, 2919, 2853, 2692, 2585, 1479, 1260; ^{1}H NMR (δ ppm): 8.50 (br s, 2H, NH$_2^+$); 7.01–6.99 (m, 2H, Ar–H); 6.92–6.87 (m, 1H, Ar–H); 5.36 (t, *J* = 5.1; 1H, OH); 3.89–3.86 (m, 2H, Ar–O–CH$_2$); 3.79–3.74 (m, 4H, Ar–O–CH$_2$–C*H*$_2$–O–C*H*$_2$–CH$_2$–NH); 3.64–3.58 (m, 1H, C*H*H–OH); 3.52–3.44 (m, 1H, CH*H*–OH); 3.32–3.23 (m, 1H, NH–C*H*); 3.14 (t, 2H, *J* = 5.6. O–CH$_2$–C*H*$_2$–NH); 2.20 (s, 6H, CH$_3$–Ar); 1.70 (d, *J* = 6.7; 3H, CH–C*H*$_3$), LC–MS [M+H]$^+$ *m*/*z*: 268.34, 100%. $[\alpha]_D^{20}$ = −6.64° (CH$_3$OH, *c* 2%).

4.1.1.23. *S*-(+)-2*N*-{2-[2-(2,6-Dimethylphenoxy)ethoxy]ethyl} aminopropan-1-ol (23). White solid. Yield = 70%; *M* = 267.36; $C_{15}H_{25}NO_3$; mp 46–48 °C; [%^{calcd}/$_{analyzed}$] C$^{67.38}$/$_{67.23}$, H$^{9.42}$/$_{9.75}$, N$^{5.24}$/$_{4.99}$; ^{1}H NMR (δ ppm): 7.00 (d, *J* = 7.4; 2H, Ar–H3); 6.92 (dd, *J* = 8.1; *J* = 6.2; 1H, Ar–H4); 3.98–3.92 (m, 2H, Ar–O–CH$_2$); 3.84–3.78 (m, 2H, Ar–O–CH$_2$–C*H*$_2$); 3.74–3.67 (m, 2H, O–C*H*$_2$–CH$_2$–NH); 3.61 (dd, *J* = 10.5; *J* = 3.7; 1H, CH*H*–OH); 3.30 (dd, *J* = 11.2; *J* = 7.2; 1H, C*H*H–OH); 3.06–2.96 (m, 1H, O–CH$_2$–C*H*H–NH); 2.91–2.74 (m, 1H, O–CH$_2$–CH*H*–NH); 2.91–2.74 (m, 1H, NH–C*H*); 2.41 (br s, 2H, OH, NH); 2.29 (s, 6H, CH$_3$–Ar); 1.09 (d, *J* = 6.7; 3H, CH–C*H*$_3$); $[\alpha]_D^{20}$ = +13.07° (CH$_3$OH, *c* 2%).

*4.1.1.23.1. S-(+)-2N-{2-[2-(2,6-Dimethylphenoxy)ethoxy]ethyl} aminopropan-1-ol hydrochloride (**23a**).* White solid. Yield = 80%; *M* = 303.82; $C_{15}H_{26}NO_3Cl$; mp 97–99 °C; [%^{calcd}/$_{analyzed}$] C$^{59.29}$/$_{59.34}$, H$^{8.63}$/$_{8.80}$, N$^{4.53}$/$_{4.60}$; IR (KBr, cm^{-1}): 3411, 2927, 1628, 1476, 1202, 1128, 1052, 770; ^{1}H NMR (δ ppm): 8.77 (br s, 1H, N*H*H$^+$); 8.54 (br s, 1H, NH*H*$^+$); 7.00 (d, *J* = 7.4; 1H, Ar–H3); 6.89 (dd, *J* = 8.5; *J* = 6.5; 1H, Ar–H4); 5.37 (t, *J* = 5.3; 1H, OH); 3.90–3.87 (m, 2H, Ar–O–CH$_2$); 3.81–3.74 (m, 4H, Ar–O–CH$_2$–C*H*$_2$–O–C*H*$_2$–CH$_2$–NH); 3.63 (dt, *J* = 11.8; *J* = 4.3; 1H, O–CH$_2$–C*H*H–NH); 3.50 (dt, *J* = 11.8; *J* = 5.4; O–CH$_2$–CH*H*–NH); 3.28 (br s, 1H, NH–C*H*); 3.15 (br s, 2H, C*H*$_2$–OH); 2.21 (s, 6H, CH$_3$–Ar); 1.19 (d, *J* = 6.7; 3H, CH–C*H*$_3$). $[\alpha]_D^{20}$ = +6.36° (CH$_3$OH, *c* 2%).

4.1.1.24. *R,S*-2*N*-{2-[2-(2,6-Dimethylphenoxy)ethoxy]ethyl} aminobutan-1-ol (24). White solid. Yield = 65%; *M* = 281.39; $C_{16}H_{27}NO_3$; mp 48–50 °C; [%^{calcd}/$_{analyzed}$] C$^{68.29}$/$_{68.40}$, H$^{9.67}$/$_{10.07}$, N$^{4.98}$/$_{4.88}$; IR (KBr, cm^{-1}): 3422, 3297, 3155, 2963, 2914, 2871, 2830, 2360, 1629, 1593, 1461, 1205, 1136, 1062, 763; ^{1}H NMR (δ ppm): 7.00 (d, *J* = 7.6; 2H, Ar–H3); 6.92 (dd, *J* = 8.6; *J* = 6.5; 1H, Ar–H4); 3.96–3.92 (m, 2H, Ar–O–CH$_2$); 3.86–3.81 (m, 2H, Ar–O–CH$_2$–C*H*$_2$); 3.76 (t, *J* = 4.9; 2H, O–C*H*$_2$–CH$_2$–NH); 3.71 (dd, *J* = 11.4; *J* = 4.0; 1H, C*H*H–OH); 3.43 (dd, *J* = 11.1; *J* = 6.5; 1H, CH*H*–OH); 3.05 (dt, *J* = 12.0; *J* = 5.5; 1H, O–CH$_2$–C*H*H–NH); 2.90 (dt, *J* = 12.9; *J* = 4.6; 1H, O–CH$_2$–CH*H*–NH); 2.76–2.66 (m, 1H, NH–C*H*); 2.58 (br s, 2H, OH, NH); 2.29 (s, 6H, CH$_3$–Ar); 1.64–1.45 (m, 2H, CH–C*H*$_2$–CH$_3$); 0.95 (t, *J* = 7.7; 3H, CH–CH$_2$–C*H*$_3$).

4.1.1.25. *R*-(−)-2N-({2-[2-(2,6-Dimethylphenoxy)ethoxy]ethyl} aminobutan-1-ol (25). White solid. Yield = 65%; *M* = 281.39; $C_{16}H_{27}NO_3$; mp 50–52 °C; [%^{calcd}/$_{analyzed}$] C$^{68.29}$/$_{68.14}$, H$^{9.67}$/$_{9.66}$, N$^{4.98}$/$_{4.91}$; IR (KBr, cm^{-1}): 3294, 3131, 3021, 2964, 2922, 2870, 2834, 2570, 2398, 1459, 1203, 1129, 1064, 762; ^{1}H NMR (δ ppm): 7.05–6.97 (m, 2H, Ar–H3); 6.96–6.87 (m, 1H, Ar–H4); 3.97–3.91 (m, 2H, Ar–O–CH$_2$); 3.83–3.77 (m, 2H, Ar–O–CH$_2$–C*H*$_2$); 3.72–3.64 (m, 2H, O–C*H*$_2$–CH$_2$–NH); 3.61 (dd, *J* = 10.6; *J* = 4.0; 1H, C*H*H–OH); 3.29 (dd, *J* = 10.8; *J* = 6.4; 1H, CH*H*–OH); 2.99–2.88 (m, 1H, O–CH$_2$–C*H*H–NH); 2.81–2.71 (m, 1H, O–CH$_2$–CH*H*–NH); 2.62–2.51 (m, 1H, NH–C*H*); 2.29 (s, 6H, CH$_3$–Ar); 1.56–1.36 (m, 2H, CH–C*H*$_2$–CH$_3$); 0.92 (t, *J* = 7.4; 3H, CH–CH$_2$–C*H*$_3$); $[\alpha]_D^{20}$ = −11.719° (CH$_3$OH, *c* 1%).

4.1.1.26. *S*-(+)-2*N*-{2-[2-(2,6-Dimethylphenoxy)ethoxy]ethyl} aminobutan-1-ol (26). White solid. Yield = 75%; *M* = 281.39; $C_{16}H_{27}NO_3$; mp 51–53 °C; [%^{calcd}/$_{analyzed}$] C$^{68.29}$/$_{67.83}$, H$^{9.67}$/$_{9.78}$, N$^{4.98}$/$_{4.91}$; ^{1}H NMR (δ ppm): 7.00 (d, *J* = 7.6; 2H, Ar–H3); 6.92 (dd, *J* = 8.6; *J* = 6.5; 1H, Ar–H4); 3.96–3.92 (m, 2H, Ar–O–CH$_2$); 3.86–3.81 (m, 2H, Ar–O–CH$_2$–C*H*$_2$); 3.72 (t, *J* = 4.9; 2H, O–C*H*$_2$–CH$_2$–NH); 3.67 (dd, *J* = 11.4; *J* = 4.0; 1H, C*H*H–OH); 3.37 (dd, *J* = 11.2; *J* = 6.7; 1H, CH*H*–OH); 3.00 (m, 1H, O–CH$_2$–C*H*H–NH); 2.90 (dt, *J* = 12.5; *J* = 4.5; 1H, O–CH$_2$–CH*H*–NH); 2.76–2.66 (m, 1H, NH–C*H*); 2.58 (br s, 2H, OH, NH); 2.29 (s, 6H, CH$_3$–Ar); 1.64–1.45 (m, 2H, CH–C*H*$_2$–CH$_3$); 0.95 (t, *J* = 8.2; 3H, CH–CH$_2$–C*H*$_3$); $[\alpha]_D^{20}$ = +11.660° (CH$_3$OH, *c* 1%).

4.1.1.27. D,L-*trans*-2*N*-{2-[2-(2,6-Dimethylphenoxy)ethoxy] ethyl}aminocyclohexan-1-ol (27). White solid. Yield = 60%; *M* = 307.43; $C_{18}H_{29}NO_3$; mp 47–49 °C; [%^{calcd}/$_{analyzed}$] C$^{70.32}$/$_{70.98}$, H$^{9.51}$/$_{9.53}$, N$^{4.56}$/$_{4.51}$; IR (KBr, cm^{-1}): 3297, 3178, 3022, 2954, 2921, 2852, 2832, 2664, 1591, 1477, 1205, 1119, 1083, 775, 405; ^{1}H NMR (δ ppm): 7.01–6.89 (m, 3H, Ar–H); 3.95–3.92 (m, 2H, Ar–O–CH$_2$); 3.81–3.79 (m, 2H, Ar–O–CH$_2$–C*H*$_2$); 3.69–3.66 (m, 2H, C*H*$_2$–CH$_2$–NH); 3.18–3.12 (m, 1H, C*H*–OH); 3.12–3.03 (m, 1H, CH*H*–NH); 2.72–2.65 (m, 1H, O–CH$_2$–CH*H*–NH); 2.29 (s, 6H, CH$_3$–Ar); 2.27–2.19 (m, 1H, NH); 2.11–2.02 (m, 2H, cyclohex); 1.74–1.69 (m, 2H, cyclohex); 1.24–1.29 (m, 4H, cyclohex).

4.1.1.28. 1*N*-{2-[2-(2,6-Dimethylphenoxy)ethoxy]ethyl}piperidin-4-ol (28). White solid. Yield = 55%; *M* = 293.40; $C_{17}H_{27}NO_3$; mp 51–53 °C; [%^{calcd}/$_{analyzed}$] C$^{69.59}$/$_{69.41}$, H$^{9.28}$/$_{9.23}$, N$^{4.77}$/$_{4.75}$; IR (KBr, cm^{-1}): 3434, 3288, 2947, 2930, 2888, 2870, 2810, 2360, 2341, 1475, 1201, 1079, 781, 766; ^{1}H NMR (δ ppm): 7.02–6.97 (m, 2H, Ar–H3); 6.94–6.88 (m, 1H, Ar–H4); 3.96–3.89 (m, 2H, Ar–O–CH$_2$); 3.81–3.76 (m, 2H, Ar–O–CH$_2$–C*H*$_2$); 3.70 (t, *J* = 5.7; C*H*H–CH$_2$–NH); 3.72–3.68 (m, 1H, C*H*–OH); 2.91–2.79 (m, 2H, N–CH$_2$(-pip)); 2.64 (t, 2H, *J* = 5.7; CH$_2$–C*H*$_2$–NH); 2.28 (s, 6H, CH$_3$–Ar); 2.27–2.17 (m, 2H, N–CH$_2$(pip)); 1.96–1.84 (m, 2H, CH$_2$(pip)); 1.69–1.53 (m, 2H, CH$_2$(pip)).

4.1.1.29. *R,S*-2*N*-{2-[2-(2,4,6-Trimethylphenoxy)ethoxy]ethyl} aminopropan-1-ol (29). White solid. Yield = 50%; *M* = 281.39; $C_{16}H_{27}NO_3$; mp 53–55 °C; [%^{calcd}/$_{analyzed}$] C$^{68.29}$/$_{68.29}$, H$^{9.67}$/$_{9.61}$, N$^{4.98}$/$_{4.86}$; IR (KBr, cm^{-1}): 3429, 3293, 3158, 2962, 2912, 2835, 1637, 1459, 1216, 1135, 1062, 883; ^{1}H NMR (δ ppm): 6.81 (s, 2H, Ar–H); 3.97–3.86 (m, 2H, Ar–O–CH$_2$); 3.83–3.75 (m, 2H, Ar–O–CH$_2$–CH$_2$); 3.72–3.63 (m, 2H, O–C*H*$_2$–CH$_2$–NH); 3.58 (dd, *J* = 10.5; *J* = 4.1; 1H, CH*H*–OH); 3.25 (dd, *J* = 10.6; *J* = 6.8; 1H, C*H*H–OH); 3.05–2.89 (m, 1H, O–CH$_2$–C*H*H–NH); 2.86–2.68 (m, 2H, O–CH$_2$–CH*H*–NH + C*H*–CH$_2$–OH); 2.25 (s, 6H, CH$_3$–Ar); 2.23 (s, 3H, CH$_3$–Ar); 1.05 (d, *J* = 6.7; 3H, CH–C*H*$_3$).

4.1.1.30. D,L-*trans*-2*N*-{2-[2-(2,4,6-Trimethylphenoxy)ethoxy] ethyl}aminocyclohexan-1-ol (30). White solid. Yield = 55%; *M* = 321.45; $C_{19}H_{31}NO_3$; mp 54–56 °C; [%^{calcd}/$_{analyzed}$] C$^{70.93}$/$_{70.90}$, H$^{9.72}$/$_{9.53}$, N$^{4.36}$/$_{4.35}$; IR (KBr, cm^{-1}): 3424, 3300, 3158, 3001, 2928, 2858, 2362, 1636, 1484, 1456, 1217, 1122, 1060, 904, 856, 590; ^{1}H NMR (δ ppm): 6.81 (s, 2H, Ar–H); 3.94–3.87 (m, 2H,

Ar–O–CH_2); 3.81–3.75 (m, 2H, Ar–O–CH_2–CH_2); 3.70–3.62 (m, 2H, O–CH_2–CH_2–NH); 3.44 (br s, 1H, NH); 3.23–3.11 (m, 1H, *CH*–OH); 3.11–3.00 (m, 1H, O–CH_2–*CH*H–NH); 2.67 (dt, J = 12.2; J = 4.6; 1H, O–CH_2–CH*H*–NH); 2.25 (s, 6H, CH_3–Ar); 2.23 (s, 3H, CH_3–Ar); 2.22–2.16 (m, 1H, C*H*–NH); 2.12–1.98 (m, 2H, cyclohex); 1.77–1.66 (m, 2H, cyclohex); 1.35–1.17 (m, 3H, cyclohex); 1.06–0.91 (m, 1H, cyclohex).

Data for single crystal were collected at 120 K using the Oxford Diffraction SuperNova four circle diffractometer, equipped with the Cu (1.54184 Å) Kα radiation source, graphite monochromator and Oxford CryoJet system for measurements at low temperature. The structure was solved by direct methods using SIR-97[18] and all non–hydrogen atoms were refined anisotropically using weighted full-matrix least-squares on F^2. Refinement and further calculations were carried out using Shelxl-97.[19] The hydrogen atoms bonded to carbon atoms were included in the structure at idealized positions and were refined using a riding model with U_{iso}(H) fixed at 1.2 U_{eq} of C and 1.5 U_{eq} for methyl groups. Hydrogen atoms attached to oxygen and nitrogen atoms were found from the difference Fourier map and refined without any restraints. For molecular graphics ORTEP[20] and MERCURY[21] programs were used.

$C_{12}H_{26}ClNO_3$, M_r = 308.82, crystal size = 0.45 × 0.40 × 0.27 mm^3, monoclinic, space group $P2_1$, a = 7.7258(1) Å, b = 7.2259(1) Å, c = 14.792(2) Å, V = 812.56(2) $Å^3$, Z = 2, T = 120(2) K, 9314 reflections collected, 3031 unique reflections (R_{int} = 0.0333), $R1$ = 0.0343, $wR2$ = 0.0938 [$I > 2\sigma(I)$].

CCDC 1431730 contains the supplementary crystallographic data. These data can be obtained free of charge from The Cambridge Crystallographic Data Centre via www.ccdc.cam.ac.uk/data_request/cif.

The liquid chromatography separation of the analytes was done using an Agilent 1100 (Agilent Technologies, Waldbronn, Germany) LC system. The mass spectrometric analyses were performed on an Applied Biosystems MDS Sciex (Concord, Ontario, Canada) API 2000 triple quadrupole mass spectrometer equipped with an electrospray ionization interface and operated in the positive ionization mode. The data acquisition and processing were done by using the Applied Biosystems Analyst software, version 1.4.2. The injected volume of the analytes solutions were 10 μL at the concentration of 250 ng/mL in methanol.

The chromatographic separation of the analytes was carried out on a Chiralcel OD-RH analytical column (250 mm × 4.6 mm, 5 μm) from Daicel Chemical Industries (Tokyo, Japan). The optimized separation resolution for the compounds was achieved at 30 °C column temperature with a flow rate of the mobile phase 0.4 mL/min containing acetonitrile and water (60:40, v/v) with an addition of 0.01% formic acid.

The ion source parameters were set to: 5500 V ion spray voltage, 40 psi the nebulizer gas pressure, 35 psi the turbo gas pressure, 400 °C the heated nebulizer temperature, and 10 psi the curtain gas pressure. With the unit mass resolution, the mass spectrometer was operated in the multiple reaction monitoring mode (MRM), by monitoring the transitions of m/z 268.2 → 250.3.

4.2. Pharmacology

Antiepileptic activity and neurological toxicity assays were carried out by the Antiepileptic Drug Development Program, Epilepsy Branch, National Institute of Neurological and Communicative Disorders and Stroke, National Institute of Health in Rockville, USA.[15] Compounds were injected as suspensions in 0.5% methylcellulose at three dosage levels (30, 100 and 300 mg/kg b.w.) intraperitoneally (*ip*) into mice, and orally. The preliminary evaluation was a qualitative assay which used small groups of animals (1–8) and included three tests: maximal electroshock seizure (MES), subcutaneous pentylenetetrazol (ScMet), and neurotoxicity (rotarod), noted at 30 min and 4 h after administration.[22] The MES were elicited by 60 Hz alternating current at 50 mA (mice) or 150 mA (rats) delivered for 0.2 s via corneal electrodes. A drop of 0.9% NaCl solution was placed into each eye prior to applying the electrodes. Protection in the MES test was defined as the abolition of the hindlimb tonic extension component of the seizure. The ScMet was conducted by administration 85 mg/kg of pentylenetetrazole dissolved in 0.9% NaCl solution into the posterior midline of mice. A minimal time of 30 min subsequent to subcutaneous administration of pentylenetetrazole was used for seizure detection. A failure to observe even a threshold seizure (a single episode of clonic spasm of at least 5 s in duration) was regarded as protection. Neurological deficit was measured in mice by the rotarod test. The mouse was placed on a 1 in. diameter knurled plastic rod rotating at 6 rpm. Neurotoxicity was indicated by the inability of the animal to maintain equilibrium on the rod for at least 1 min in each of the three trials. In rats, neurological deficit was indicated by ataxia and loss of placing response and muscle tone.

The 6 Hz model test was carried out according to the protocol originally described by Brown et al.[23] and more recently by Barton et al.[14] and Kaminski et al.[24] Corneal stimulation (0.2 ms duration monopolar rectangular pulses at 6 Hz for 3 s) was delivered by a constant current device. During the stimulation, mice were manually restrained and released into the observation cage immediately after application of current. The seizures were often preceded by a brief period of intense locomotor agitation. The animals then exhibited a 'stunned' posture associated with rearing, forelimb automatic movements and clonus, twitching of the vibrissae, and Straub-tail. The duration of the seizure activity ranged from 60 to 120 s in untreated animals. In the end of the seizure, animals resumed their normal exploratory behavior. The experimental endpoint was protection against the seizure. The animal was considered to be protected if it resumed its normal exploratory behavior within 10 s from the stimulation. The pilocarpine test involves determination whether the investigated compound can halt acute pilocarpine-induced status. A challenge dose of pilocarpine (50 mg/kg) is administered *ip* and animals are observed until the first convulsive (e.g., stages 3, 4, or 5) seizure (time zero). The seizure severity is determined using the Racine scale.[25] At this point a minimally toxic dose of the candidate drug is administered to a group of 8 male albino Sprague Dawley rats (150–180 g) *ip* Efficacy is defined by the ability of an investigational drug to halt the further expression of pilocarpine induced convulsive seizures (*e.g.* stages 3, 4, or 5). Anticonvulsant quantification, that is the doses of drug required to cause the biological responses in 50% of animals (ED_{50}), and the respective 95% confidence intervals, were determined for selected compounds displaying sufficient anticonvulsant activity and low neurotoxicity in the above primary evaluations, by means of a computer program using probit analysis.

Formalin test is conducted in mice. The test covers the administration of formalin to hindlimb of the animal, which causes the licking of the place of administration. The total time of licking is considered as corresponding to the intensity of pain sensation experienced by the animal. It is characteristic, that there are two phases of the test. The first phase (acute) is about 10 min long and corresponds to the direct stimulation of peripheral sensor and pain neurons. The second phase (inflammatory) develops as the response of liberation of inflammatory mediators from impaired tissues and nerves' endings. The activity in that phase corresponds with beneficial effect in neuropathic pain. Simultaneously control tests are performed which involve administration to other animals solvent alone (*e.g.* methylcellulose). The shortening of the time of hindlimb licking is scored as analgesic activity.[26]

Receptor binding studies for **22a** and **23a** have been performed as standard high throughput profile at Cerep (France). Results showing an inhibition (or stimulation for assays run in basal

conditions) higher than 50% are considered to represent significant effects of the test compounds. 50% is the most common cut-off value for further investigation (determination of IC_{50} or EC_{50} values from concentration–response curves) that would be recommended. Results showing an inhibition (or stimulation) between 25% and 50% are indicative of weak to moderate effects. Results showing an inhibition (or stimulation) lower than 25% are not considered significant and mostly attributable to variability of the signal around the control level. Low to moderate negative values have no real meaning and are attributable to variability of the signal around the control level. High negative values ($\geqslant$50%) that are sometimes obtained with high concentrations of test compounds are generally attributable to non-specific effects of the test compounds in the assays. On rare occasion they could suggest an allosteric effect of the test compound.

4.3. Mutagenicity or antimutagenicity assay

Mutagenicity assay was performed according to previously described procedure.[27,28] Briefly, for the *V. harveyi* mutagenicity test, 10 μL of test compound was added to exponentially growing cultures (A_{600} = 0.1, 30 °C) and incubation was continued until the OD_{600} had increased to 0.3–0.4. Then, 5×10^6 bacterial cells were spread onto BOSS agar plates containing neomycin at a final concentration of 100 μg/mL. Plates were incubated for 48 h at 30 °C and neomycin-resistant colonies were counted manually. All the assays were carried out in triplicate.

In the antimutagenicity assay performed with the *V. harveyi* strains, 10 μL of test compound was added to exponentially growing cultures (A_{600} = 0.1, 30 °C) and incubation was continued for 15 min. Then, 10 μL of NQNO was added to samples with tested compounds and cultivation was continued till A_{600} between 0.3 and 0.4 to mid-log phase of growth. Next, 5×10^6 bacterial cells grown in BOSS medium were transferred onto BOSS plates. Following 48 h incubation at 30 °C, neomycin-resistant colonies were counted.[29] All experiments were analyzed in three independent repetitions.

4.4. Metabolic stability

Mouse liver microsomes (MLMs), glucose-6-phosphate, NADP, glucose-6-phosphate dehydrogenase and levallorphan were supplied by Sigma Aldrich.

Mouse liver microsomal incubations were conducted in duplicate. Incubations were composed of test compound (20 μM), MLMs (0.4 mg/mL), NADPH-regenerating system and potassium phosphate buffer (100 mM, pH 7.4). NADPH-regenerating system contained NADP, glucose-6-phosphate, glucose-6-phosphate dehydrogenase and potassium phosphate buffer (100 mM, pH 7.4). Firstly, the mixtures containing microsomes, test compound and buffer were preincubated at 37 °C for 15 min before the addition of NADPH-regenerating system. The resulting mixture was incubated for different time points (5, 15, 30, 60 and 90 min) at 37 °C. Next, levallorphan (20 μM, internal standard) was added, and the reaction was quenched by addition of perchloric acid (69–72%, by volume). The solution was then centrifuged to sediment the precipitates. Supernatant analysis was performed using UPLC/MS (Waters Corporation, Milford, MA, USA). For control samples NADPH-regenerating system was replaced with phosphate buffer.[30–32] The in vitro half times ($t_{1/2}$) for test compounds were determined from the slope of the linear regression of ln % parent compound remaining *versus* incubation time. The calculated $t_{1/2}$ was incorporated into the following equation to obtain intrinsic clearance (Cl_{int}) = (volume of incubation [μL]/protein in the incubation [mg]) × 0.693/$t_{1/2}$.[16]

4.5. Pharmacokinetics

The LC/ESI-MS/MS analysis were performed on an Applied Biosystems/MDS Sciex (Concord, Ontario, Canada) API 2000 triple quadrupole mass spectrometer equipped with an electrospray ionization interface. This instrument was coupled to an Agilent 1100 (Agilent Technologies, Waldbronn, Germany) LC system. Data acquisition and processing were accomplished using ABSciex Analyst 1.4.2 data collection and integration software.

Using an original LC/ESI-MS/MS method, a pharmacokinetic study for **22a** was carried out following its intravenous (1 mg/kg), intragastric (12.92 mg/kg) or intraperitoneal (12.92 mg/kg) administration to male CD1 mice. Mice were kept under conditions of constant temperature (21–25 °C) and relative humidity of approximately 40–65% with a standard light/dark cycle. Animals were housed in stainless steel cages with suspended wire-mesh floors (maximum of 10 mice per cage). Animals were fasted overnight and then weighed. Mice had free access to water throughout the experimental period. Animals were anesthetized with ketamine (100 mg/kg)/xylasine (10 mg/kg) and sacrificed at the following time intervals: at control (0 min) and 5, 15, 30, 60, 120 and 240 min after compound administration. Blood samples were collected into heparinized microfuge tubes. The samples were immediately centrifuged at 3500 rpm for 10 min. The plasma was separated into clean tubes and frozen at −30 °C prior to analysis, whereas brains were stored at −80 °C. Mice were sampled four at a time and one sample per animal was collected. The plasma concentrations of **22a** at different time points were expressed as mean ± SD, and the mean concentration–time curves were plotted. All animal experiments were performed in accordance with the institutional guidelines and were approved by the Animal Care and Ethics Committee of the Jagiellonian University.

All data in pharmacokinetic experiments were processed with the pharmacokinetic software Phoenix WinNonlin (Certara, USA). The non-compartmental pharmacokinetic parameters of $t_{1/2}$, MRT, AUC, Cl_t and V_{ss} were calculated based on moment methods. First order elimination rate constant (λ_z) was calculated by linear regression of time versus log concentration according to the Eq. 1.

$$\lambda_z = -2.303\ a \tag{1}$$

where a is a slope of a line.

The terminal half-life ($t_{1/2}$) was calculated as:

$$t_{1/2} = \frac{0.693}{\lambda_z} \tag{2}$$

For each compound, the area under the mean serum and tissue drug concentration versus time curve extrapolated to infinity ($AUC_{0\to\infty}$) was estimated using the log-linear trapezoidal rule (Eq. 3), where C_n is the concentration of last sampling.

$$AUC_{0\to\infty} = \sum_{i=1}^{n}\left(\frac{C_i + C_{i+1}}{2}\right)\cdot(t_{i+1} - t_i) + \frac{C_n}{\lambda_z} \tag{3}$$

The area under the first-moment curve ($AUMC_{0\to\infty}$) was estimated by calculation of the total area under the first-moment curve and extrapolated area using the Eq. 4, where t_n is the time of last sampling.

$$AUMC_{0\to\infty} = \sum_{i=1}^{n}\left(\frac{t_i\cdot C_i + t_{i+1}\cdot C_{i+1}}{2}\right)\cdot(t_{i+1} - t_i) + \frac{t_n\cdot C_n}{\lambda_z} + \frac{C_n}{\lambda_z^2} \tag{4}$$

Mean residence time (MRT) was calculated as:

$$MRT = \frac{AUMC_{0\to\infty}}{AUC_{0\to\infty}} \tag{5}$$

Total clearance (Cl_t) was calculated as:

$$Cl_t = \frac{D_{iv}}{AUC_{0\to\infty}} \quad (6)$$

Volume of distribution at steady state (V_{ss}) was calculated as:

$$V_d = \frac{D_{iv} \cdot AUMC_{0\to\infty}}{(AUC_{0\to\infty})^2} \quad (7)$$

where D_{iv} is an intravenous dose, AUMC is the area under the first moment curve, and AUC is the area under the zero moment curve.

The absolute bioavailability (F) of **22a** after the extravascular (ev) administration compared to the intravenous (iv) route was calculated as follows:

$$F = \frac{AUC_{ev}}{AUC_{iv}} 100\%. \quad (8)$$

Acknowledgements

The authors thank Professor Jeff Jiang, Professor James Stables, Professor Steve White, Professor Harvey Kupferberg, and dr. Tracy Chen from National Institute of Neurological Disorders and Stroke (NIH, Rockville, USA) for providing the results of anticonvulsant evaluation, as well as Professor Katarzyna Kieć-Kononowicz for coordination of the cooperation with the Faculty of Pharmacy at Jagiellonian University Medical College.

The research was co-financed by European Regional Development Fund within the Innovative Economy Program and by Jagiellonian University Medical College funding no. K/ZDS/005487.

Supplementary data

Supplementary data associated with this article can be found, in the online version, at http://dx.doi.org/10.1016/j.bmc.2016.03.006. These data include MOL files and InChiKeys of the most important compounds described in this article.

References and notes

1. Sander, J. W. *Curr. Opin. Neurol.* **2003**, *16*, 165.
2. Waszkielewicz, A.; Gunia, A.; Słoczyńska, K.; Marona, H. *Curr. Med. Chem.* **2011**, *18*, 4344.
3. Chew, C.; Collett, J.; Singh, B. *Drugs* **1979**, *17*, 161.
4. Fischer, W. *Seizure J. Br. Epilepsy Assoc.* **2002**, *11*, 285.
5. Alexander, G. J.; Kopeloff, L. M.; Alexander, R. B.; Chatterjie, N. *Neurobehav. Toxicol. Teratol.* **1986**, *8*, 231.
6. Marona, H.; Antkiewicz-Michaluk, L. *Acta Pol. Pharm.* **1998**, *55*, 487.
7. Pękala, E.; Waszkielewicz, A. M.; Szneler, E.; Walczak, M.; Marona, H. *Bioorg. Med. Chem.* **2011**, *19*, 6927.
8. Waszkielewicz, A. M.; Cegła, M.; Żesławska, E.; Nitek, W.; Słoczyńska, K.; Marona, H. *Bioorg. Med. Chem.* **2015**, *23*, 4197.
9. Waszkielewicz, A. M.; Pytka, K.; Rapacz, A.; Wełna, E.; Jarzyna, M.; Satała, G.; Bojarski, A.; Sapa, J.; Żmudzki, P.; Filipek, B.; Marona, H. *Chem. Biol. Drug Des.* **2015**, *85*, 326.
10. Russo, E.; Citraro, R.; Scicchitano, F.; De Fazio, S.; Perrota, I.; Di Paola, E. D.; Constanti, A.; De Sarro, G. *Epilepsia* **2011**, *52*, 1341.
11. Waszkielewicz, A.M.; Gunia, A.; Marona, H., WO 2,015,020,545 A2, 2013.
12. Augstein, J.; Austin, W.; Boscott, R.; Green, S.; Worthing, C. *J. Med. Chem.* **1965**, *8*, 356.
13. Sivý, J.; Kettmann, V.; Frešová, E. *Acta Crystallogr., Sect. C* **1991**, *47*, 2695.
14. Barton, M. E.; Klein, B. D.; Wolf, H. H.; White, H. S. *Epilepsy Res.* **2001**, *47*, 217.
15. Stables, J. P.; Kupferberg, H. J. Molecular and Cellular Targets for Anti-epileptic Drugs In In Avanzini, G., Regesta, P., Tanganelli, A., Avoli, M., Eds.; John Libbey & Company Ltd: London, 1997; Vol. 23129, p 191.
16. Singh, J. K.; Solanki, A.; Shirsath, V. S. *J. Drug Metab. Toxicol.* **2012**, *3*, 1.
17. Newman, P. In *Amines*; Optical Resolution Information Center, Manhattan College Riverdale: New York, 1984; Vol. 1,
18. Altomare, A.; Burla, M. C.; Camalli, M.; Cascarano, G. L.; Giacovazzo, C.; Guagliardi, A.; Moliterni, A. G. G.; Polidori, G.; Spagna, R. *J. Appl. Crystallogr.* **1999**, *32*, 115.
19. Sheldrick, G. M. *Acta Crystallogr., Sect. A* **2008**, *64*, 112.
20. Farrugia, L. J. *J. Appl. Crystallogr.* **1997**, *30*, 565.
21. Macrae, C. F.; Edgington, P. R.; McCabe, P.; Pidcock, E.; Shields, G. P.; Taylor, R.; Towler, M.; van de Streek, J. *J. Appl. Crystallogr.* **2006**, *39*, 453.
22. White, S. H.; Woodhead, J. H.; Wilcox, K. S.; Kupferberg, H. J.; Wolf, H. H. In *Antiepileptic Drugs*; Levy, R. H., Mattson, R. H., Meldrum, B. S., Perrucca, E., Eds., 5th ed.; Lippincott Williams & Wilkins: Philadelphia, 2002; p 36.
23. Brown, W.; Schiffman, D. *J. Pharmacol. Exp. Ther.* **1953**, *107*, 273.
24. Kaminski, R. M.; Livingood, M. R.; Rogawski, M. *Epilepsia* **2004**, *45*, 864.
25. Racine, R. J. *Electroencephalogr. Clin. Neurophysiol.* **1972**, *32*, 281.
26. Capone, F.; Aloisi, A. M. *Ann. Ist. Super. Sanita* **2004**, *40*, 223.
27. Czyż, A.; Jasiecki, J.; Bogdan, A.; Szpilewska, H.; Węgrzyn, G. *Appl. Environ. Microbiol.* **2000**, *66*, 599.
28. Pekala, E.; Liana, P.; Kubowicz, P.; Powroźnik, B.; Obniska, J.; Chlebek, I.; Wegrzyn, A.; Wegrzyn, G. *Mutat. Res. Genet. Toxicol. Environ. Mutagen* **2013**, *758*, 18.
29. Słoczyńska, K.; Pekala, E.; Wajda, A.; Wegrzyn, G.; Marona, H. *Lett. Appl. Microbiol.* **2010**, *50*, 252.
30. Hamelin, B. A.; Bouayad, A.; Drolet, B.; Gravel, A.; Turgeon, J. *Drug Metab. Dispos.* **1998**, *26*, 536.
31. Di, L. *J. Biomol. Screening* **2003**, *8*, 453.
32. Huang, J.; Si, L.; Fan, Z.; Hu, L.; Qiu, J.; Li, G. *J. Chromatogr., Sect. B* **2011**, *879*, 3386.